Spatial and Temporal Variability in Concentration-Discharge Relationships at the Event Scale

A. Musolff, Q. Zhan, Rémi Dupas, C. Minaudo, J. Fleckenstein, M. Rode, J. Dehaspe, K. Rinke

Water Resources Research

RESEARCH ARTICLE
10.1029/2020WR029442

Spatial and Temporal Variability in Concentration-Discharge Relationships at the Event Scale

A. Musolff[1], Q. Zhan[2,3], R. Dupas[4], C. Minaudo[5], J. H. Fleckenstein[1,6], M. Rode[7,8], J. Dehaspe[1], and K. Rinke[3]

[1]Department of Hydrogeology, UFZ - Helmholtz-Centre for Environmental Research GmbH, Leipzig, Germany, [2]Netherlands Institute of Ecology (NIOO-KNAW), Wageningen, the Netherlands, [3]Department of Lake Research, UFZ - Helmholtz-Centre for Environmental Research GmbH, Magdeburg, Germany, [4]UMR SAS, INRAE, Institut Agro, Rennes, France, [5]Physics of Aquatic Systems Laboratory, Margaretha Kamprad Chair, EPFL-APHYS, Lausanne, Switzerland, [6]Bayreuth Centre of Ecology and Environmental Research (BayCEER), University of Bayreuth, Bayreuth, Germany, [7]Department of Aquatic Ecosystem Analysis, UFZ - Helmholtz-Centre for Environmental Research GmbH, Magdeburg, Germany, [8]Institute of Environmental Science and Geography, University of Potsdam, Potsdam-Golm, Germany

Key Points:

- We compare event-scale and inter-annual concentration-discharge relationships in four adjoined catchments with contrasting land use
- The variability of event-scale C-Q relationships was shaped by land use and antecedent conditions for biogeochemically reactive but not for geogenic solutes
- For biogeochemically reactive solutes, event-scale C-Q patterns can contrast the inter-annual pattern obtained from all observations

Supporting Information:

Supporting Information may be found in the online version of this article.

Correspondence to:

A. Musolff,
andreas.musolff@ufz.de

Citation:

Musolff, A., Zhan, Q., Dupas, R., Minaudo, C., Fleckenstein, J. H., Rode, M., et al. (2021). Spatial and temporal variability in concentration-discharge relationships at the event scale. *Water Resources Research*, *57*, e2020WR029442. https://doi.org/10.1029/2020WR029442

Received 11 DEC 2020
Accepted 23 SEP 2021

Abstract The analysis of concentration-discharge (C-Q) relationships from low-frequency observations is commonly used to assess solute sources, mobilization, and reactive transport processes at the catchment scale. High-frequency concentration measurements are increasingly available and offer additional insights into event-scale export dynamics. However, only few studies have integrated inter-annual and event-scale C-Q relationships. Here, we analyze high-frequency measurements of specific conductance (EC), nitrate (NO_3-N) concentrations and spectral absorbance at 254 nm (SAC_{254}, as a proxy for dissolved organic carbon) over a two year period for four neighboring catchments in Germany ranging from more pristine forested to agriculturally managed settings. We apply an integrated method that adds a hysteresis term to the established power law C-Q model so that concentration intercept, C-Q slope and hysteresis can be characterized simultaneously. We found that inter-event variability in C-Q hysteresis and slope were most pronounced for SAC_{254} in all catchments and for NO_3-N in forested catchments. SAC_{254} and NO_3-N event responses in the smallest forested catchment were closely coupled and explainable by antecedent conditions that hint to a common near-stream source. In contrast, the event-scale C-Q patterns of EC in all catchments and of NO_3-N in the agricultural catchment without buffer zones around streams were less variable and similar to the inter-annual C-Q relationship indicating a homogeneity of mobilization processes over time. Event-scale C-Q analysis thus added key insights into catchment functioning whenever the inter-annual C-Q relationship contrasted with event-scale responses. Analyzing long-term and event-scale behavior in one coherent framework helps to disentangle these scattered C-Q patterns.

1. Introduction

Anthropogenic activities such as intensive agriculture and waste water discharge deteriorate the quality of water resources. More specifically, anthropogenic sources increase the aquatic concentration and fluxes of nutrients like nitrogen, phosphorus and organic carbon, leading to eutrophication in rivers, lakes and coastal waters (Carpenter et al., 2011; Schlesinger, 2009). This can pose a threat to water security and downstream aquatic ecosystem health and functioning (Foley et al., 2005). For effective catchment-scale water quality management, knowledge on sources, pathways and reaction processes of critical constituents is needed. Reactive transport at the catchment scale, is however, complex and tends to span a large range of spatial and temporal scales (Gall et al., 2013; Kirchner, 2003; Sivapalan, 2006). This often hinders establishing a unique cause-effect relationship.

One way of approaching this complexity involves the analysis of the integrated response of concentration (C) of a constituent and discharge (Q) at a given point in the stream to identify underlying processes and their hierarchy (Basu et al., 2011; Godsey et al., 2009; Musolff et al., 2015). More specifically, characterizing the relationship between concentration and discharge proved valuable to link temporal patterns in the data to dominant processes at the catchment scale (Sivapalan, 2006). This link may however not always be fully

identifiable as several processes can lead to similar observable patterns (Musolff et al., 2017a). The processes that shape C-Q relationships are a consequence of solute availability and hydrological connectivity in source zones (Dupas et al., 2015; Werner et al., 2019; Winterdahl et al., 2011), source zone distribution in the catchment (Ameli et al., 2017; Dupas et al., 2019; Musolff et al., 2017a; Seibert et al., 2009; Zhi et al., 2019), reactions along subsurface flow paths (Musolff et al., 2017a; van der Velde et al., 2010; Yang et al., 2018) and in the stream network (Koenig et al., 2017; Moatar et al., 2017; Wollheim et al., 2017). C-Q relationships have been used to identify processes at different temporal scales: long-term average behavior (Basu et al., 2010; Musolff et al., 2015; Zarnetske et al., 2018), long-term changes of sources (Ehrhardt et al., 2019; Moatar et al., 2017; Westphal et al., 2020), seasonal changes (Koenig et al., 2017; Minaudo et al., 2019; Winterdahl et al., 2011) and changes at the runoff event time scale (Fovet et al., 2018; Knapp et al., 2020; Strohmeier et al., 2013; Vaughan et al., 2017; Werner et al., 2019). Runoff events are of special interest for catchment-scale assessments as they are critical moments of mobilization and export (Knapp et al., 2020; Werner et al., 2019) and often dominate the total load (Birkel et al., 2017).

C-Q relationships are most often described by power law models in the form $C = aQ^b$ with a defining the concentration level and exponent b defining the direction and strength of concentration changes with Q. For the latter, we distinguish dilution ($b < 0$) from enrichment ($b > 0$) and neutral ($b \sim 0$) C-Q patterns (Godsey et al., 2009; Musolff et al., 2015). However, at the scale of runoff events, hysteresis between concentration and discharge is often observed (Bieroza & Heathwaite, 2015; Evans & Davies, 1998) that cannot be captured by the power law formulation. Hysteresis results from systematic differences of concentration for the same discharge depending on the position on the event hydrograph (rising or falling limb). This behavior is explained by the mixing of different runoff sources with a different timing (e.g., base flow, interflow and event flow (Evans & Davies, 1998)) or an early or late activation of sources during the event. For dissolved constituents this results from the spatial arrangement and connectivity of the sources (Strohmeier et al., 2013), biogeochemical reactions in the source zone during the course of an event (Bao et al., 2017) or the exhaustion of a source during the event (Duncan et al., 2017; Sebestyen et al., 2008). By that, hysteresis and event-scale C-Q responses are shaped by land use and anthropogenic impacts as well as by the interplaying hydroclimatic-conditions (Burns et al., 2019; Butturini et al., 2008; Knapp et al., 2020; Vaughan et al., 2017). Hysteretic C-Q relationships are classified in terms of their direction into clockwise (CW), counterclockwise (CCW) and complex (e.g., eight-shaped) patterns (Burns et al., 2019; Evans & Davies, 1998). This type of analyses needs high frequency measurements of concentration and discharge and allow insights into the availability and the release of solutes from catchments (Kirchner et al., 2004). Here, deriving metrics to characterize single C-Q events and classifying the response such as hysteresis and flushing indices are a common approaches for this type of analysis (Lloyd et al., 2016; Vaughan et al., 2017).

High-frequency water chemistry data measured in-situ have been previously the bottleneck of extensive event-scale analyses (Kirchner et al., 2004) but now have become more available (Rode, Wade, et al., 2016; von Freyberg et al., 2017). Today, a growing number of studies (Burns et al., 2019) utilize high-frequency concentration measurements to investigate event-scale solute mobilization under different degrees of human impacts, unveiling source availability and limitation, source location and source connectivity, and reactive transport processes. These processes, however, can also be approached by the C-Q analysis of conventional low-frequency monitoring at inter-annual scale (Godsey et al., 2009; Moatar et al., 2017; Musolff et al., 2015; Thompson et al., 2011). But how do both types of analyses align and in which cases may event-analysis provide a deeper insight into reactive solute transport at catchment scale compared to inter-annual C-Q analysis? This concurs with the question of how event-scale, often hysteretic C-Q relationships aggregate to form an inter-annual C-Q relationship. There is evidence for diverging C-Q behavior comparing different time scales. For instance, intense agricultural management was shown to homogenize water flow (Boland-Brien et al., 2014) and nitrate export behavior reflected in well identifiable inter-annual C-Q relationships (Marinos et al., 2020; Musolff et al., 2017a; Thompson et al., 2011) while event-scale C-Q was found to be temporally highly variable in some cases (Lloyd et al., 2016; Vaughan et al., 2017). In case of a forested catchment Knapp et al. (2020) showed that positive C-Q relationships for nitrate at the event scale can stack up to an inter-annual dilution pattern. Similarly, DOC responses at the event scale were found to be highly variable as a result of interacting biogeochemical and hydrological processes (Blaen et al., 2017; Fovet et al., 2018; Koenig et al., 2017; Werner et al., 2019) but revealed a consistent positive inter-annual C-Q pattern. In contrast, geogenic solutes and specific conductance showed highly consistent patterns at

event-scale and inter-annual scale (Knapp et al., 2020). Although many studies used event-scale C-Q analysis and inter-annual C–Q relationships, so far only few studies integrate both types of C-Q relationships into a coherent framework (Dupas et al., 2016; Knapp et al., 2020; Minaudo et al., 2017).

Hysteresis has been characterized and quantified by comparing the concentrations on the rising and the falling limb of the event hydrograph based on a hysteresis index (Lloyd et al., 2016; Vaughan et al., 2017). As this method relies on comparing similar discharge on both sides of the hydrograph, partial events where discharge is not falling back to initial levels are difficult to analyze. Although the value in the combined information on C-Q pattern (direction) and hysteresis have been acknowledged (Dupas et al., 2016; Vaughan et al., 2017), metrics of hysteresis and patterns were mostly derived independently from each other. However, approaches to integrate hysteresis into power-law C-Q analysis at the event scale exist (House & Warwick, 1998; Krueger et al., 2009; Minaudo et al., 2017; Winter et al., 2020) but have, to the best of our knowledge, not yet been fully exploited. Advancing event-scale C-Q analysis to a mathematical framework comparable to the established inter-annual power-law approach provides an opportunity for unifying C-Q relationships across temporal scales.

In this study we hypothesize that (1) land use and its spatial arrangement in catchments determines solute-specific source location and thus lead to systematic differences in C-Q relationships. We further hypothesize that (2) antecedent hydro-climatic conditions determine variability of concentration responses to discharge at the event-scale and lead to event C-Q relationships that contrast the inter-annual behavior for biogeochemically reactive solutes, but not for geogenic solutes. To this end we analyze inter-annual and event-scale C-Q relationships in measured high-frequency in-situ time series of three water quality parameters in four neighboring catchments along a gradient of hydroclimate and anthropogenic impact. We focus on specific conductance representing geogenic solutes, and the biogeochemically reactive solutes dissolved organic carbon being of biogenic origin and nitrate being also of anthropogenic origin. To do so we utilize a coherent mathematical framework that extends the established power law C-Q analysis by integrating a hysteresis term at the event scale. We classify and compare the results across catchments, constituents, and seasons. By testing the strength of the relationships between event metrics and antecedent conditions we discuss sources and mobilization mechanisms under contrasting land use settings. Finally, we discuss the strengths and potential weaknesses of event-scale C-Q analysis compared to the established analysis at the inter-annual scale.

2. Materials and Methods

2.1. Adding Hysteresis to C-Q Analysis

The relationship of concentration C of a given solute or particulate in the stream to discharge Q is commonly described by a power law:

$$C(t) = aQ(t)^b \tag{1}$$

Here, parameter a is related to the concentration level (intercept in log-log space, concentration when $Q = 1$) while exponent b (slope in the log-log space) describes the strength and direction of the response of C to Q (Godsey et al., 2009; Jawitz &Mitchell, 2011): a positive b indicates an enrichment pattern while a negative b indicates a dilution pattern.

Several authors suggest to add a hysteresis term to this form of the C-Q relationship to be able to capture concentration deviations on the rising and falling limb (House & Warwick, 1998; Krueger et al., 2009; Minaudo et al., 2017; Winter et al., 2020). They propose the use of the derivative of discharge $dQ(t)/dt$ that allows to distinguish the rising and falling limbs of the hydrograph and thus creates a hysteresis loop around the log-log linear C-Q relationship:

$$C(t) = aQ(t)^b + c\, dQ(t)/dt \tag{2}$$

with parameter c describing the size and the direction of the hysteresis by its absolute value and its sign respectively: A positive c indicates a clockwise hysteresis while a negative c indicates a counterclockwise hysteresis. Figure 1 gives an overview over the meaning of the parameters in Equation 2. This equation can be applied on storm event time scales as well as longer timescales. However, as hysteresis patterns can change

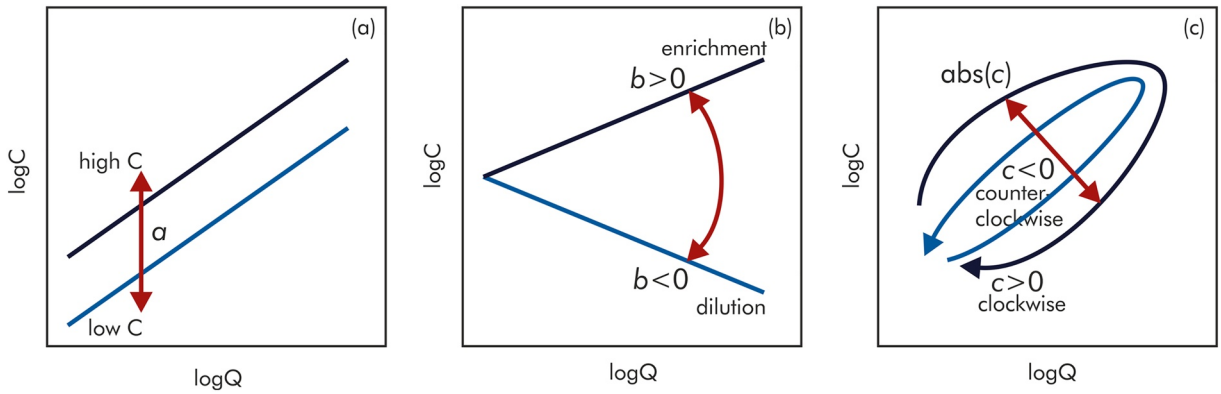

Figure 1. Meaning of model parameters *a*, *b*, and *c* in schematic C-Q plots in log-log space. abs(*c*) refers to the absolute value of *c*.

between events (Fovet et al., 2018; Lloyd et al., 2016; Vaughan et al., 2017), applications of Equation 2 at the event scale are most appropriate.

We note that parameters *a* and *c* scale with discharge and concentration (see also Jawitz and Mitchell (2011)), while parameter *b* is independent of both and thus easily transferable between catchments and solutes. That means that the event magnitude largely influences the variability of hysteresis parameter *c* between events. More specifically, an event with higher discharge but similar concentration would lead to a lower absolute value of *c*. However, with *c* we aim to describe the extent of the hysteresis and how it deviates from the log-log linear C-Q relationship. To allow for a better comparability of C-Q metrics between events, others have suggested to scale concentration and discharge prior to analysis (Lloyd et al., 2016; Vaughan et al., 2017). This affects both parameters *a* and *c*. Here we scaled $dQ(t) / dt$ by its own range such that parameter *c* is independent of the size of the specific discharge event, but we did not scale $Q(t)$ to the average event discharge or to the average inter-annual discharge. In this way, *c* describes the loop direction and relative width of hysteresis independent of the magnitude of the discharge event. Parameter *a* in Equation 2 remains equivalent to parameter *a* in the simple power law C-Q analysis (Equation 1) and captures the vertical offset of individual events as shown in Figure 1a. However, depending on the purpose of the analysis, options to scale or normalize concentration and discharge should be carefully selected prior to analysis.

2.2. Study Area

We chose four sub-catchments of the Bode river catchment in central Germany to test our approach (Figure 2). The Bode catchment is an experimental observatory for terrestrial and hydrological research within the TERENO initiative (Wollschlager et al., 2017). The chosen sub-catchments have been used in several studies on solute export regimes (Dupas et al., 2017; Musolff et al., 2015), instream processes (Rode, Halbedel, et al., 2016), nitrogen retention in reservoirs (Kong et al., 2019), DOC concentration and DOC quality dynamics (Raeke et al., 2017; Werner et al., 2019) and emerging effects of sub-catchment mixing (Winter et al., 2020). The catchments span a gradient in elevation which is linked to gradients in precipitation and land use (Table 1). While the more pristine and mainly forested catchments Warme Bode (FOR1) and upper Rappbode (FOR2) are higher in elevation and generally wetter, the catchments Hassel (AGR1) and upper Selke (AGR2) are dryer and characterized by a substantial share of arable land and grassland (Table 1). The AGR1 catchment drains into a drinking water reservoir and therefore fertilizer application in buffer zones around the streams is prohibited. All catchments are situated in the Harz Mountains and mainly underlain by metamorphic and partially igneous rocks. Note that FOR2 is a small first order catchment (2.3 km^2), while stream orders and sizes for FOR1, AGR1 and AGR2 range from 2 to 3 and 43–97 km^2, respectively.

2.3. Data Base of Concentrations and Discharge

This study mainly relies on previously published concentration and discharge data (Kong et al., 2019; Rode, Halbedel, et al., 2016; Werner et al., 2019; Winter et al., 2020). Water quality data and discharge were

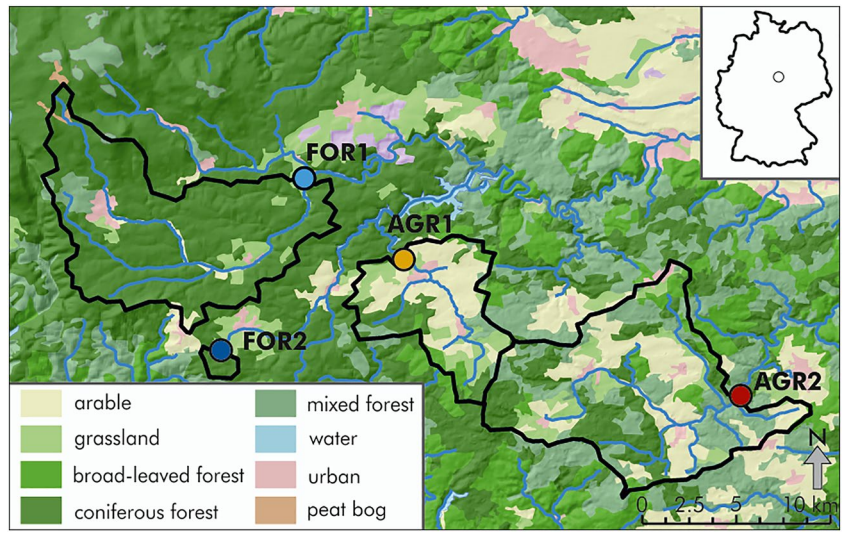

Figure 2. Land use and topography for the study catchments. Blue lines show the stream network. Inlet figure displays the location within Germany. Land use is based on Corine Land Cover (CLC, 2016).

measured every 15 min. We focused on the period between January 2013 and December 2014 where data was most consistently available for all four sites. The water quality parameters we considered in this study were nitrate-N (NO_3-N), spectral absorbance at a wavelength of 254 nm (SAC_{254}) and specific conductance (EC). Both, NO_3-N and SAC_{254} were measured using in-situ UV-VIS probes (TRIOS ProPS, Trios Germany in FOR1, AGR1 and AGR2; s::can spectrolyser, scan Austria in FOR2). We used SAC_{254} as a proxy for the part of DOC that absorbs light at 254 nm instead of estimated DOC concentrations to avoid a possible bias induced by differing internal routines of the probes to derive DOC concentration. The use of SAC_{254} as a proxy for DOC is supported by the strong relationship between SAC_{254} and lab-measured DOC concentration (see Table S1, $r_{Pearson}$ between 0.58 and 0.96). EC was measured using in-situ probes (YSI6800, YSI, USA for FOR1, AGR1 and AGR2; CTD Diver, Van Essen, Canada for FOR2). Discharge measurements relied on an established stage-discharge relationship and were provided by state authorities (LHW, 2018) (for FOR1, AGR1 and AGR2) and by Werner et al. (2019) (for FOR2). Monitoring stations were maintained every two weeks, including manual cleaning of the UV-VIS probes and grab sampling for subsequent calibration and validation with NO_3-N and DOC concentrations analyzed in the lab. Details on these procedures can be found in Rode, Halbedel, et al. (2016), Kong et al. (2019) and Werner et al. (2019). During winter times probes had to be partially removed for four weeks due to harsh weather conditions and limited site accessibility. Water temperature was recorded with the YSI and CTD probes.

Briefly, data preparation included five steps: drift corrections, outlier detection, gap filling, calibration, and moving averaging. Time series of UV-VIS based parameters tended to drift due to biofouling between the probe maintenances. This was corrected by distributing the offset between mean values one hour before and

Table 1
Overview Table With Catchment Size, Land Use, Climate and Topography Metrics for the Four Studied Catchments

Catchment	Abbr	Area	SO	P	Gr	LC_{ara}	LC_{gras}	LC_{for}	Elevation
		[km^2]	[-]	[mm a^{-1}]	[°]	[%]	[%]	[%]	[m asl]
Warme Bode	FOR1	97.15	2	1,184	4.32	2.7	4.9	89.6	585
upper Rappbode	FOR2	2.33	1	1,061	3.06	0.0	1.2	98.8	581
Hassel	AGR1	43.40	2	865	2.78	41.9	20.0	35.0	505
upper Selke	AGR2	94.53	3	698	3.91	25.7	10.3	61.4	456

Note. SO-stream order. P-mean annual precipitation (1986–2015, Cornes et al. (2018)), Gr-topographic gradient (based on 25 m DEM, EEA (2013)), LC-land cover based on CORINE Land Cover (CLC, 2016): ara-cropland, pas-pastures, for-forest. Elevation refers to the catchment mean based on 25m DEM.

after cleaning equally among the two weeks maintenance interval assuming an exponential growth. Outliers were detected with a two-step procedure. First, values outside a physically likely range were removed (see Table S2). Second, Grubbs test (Grubbs, 1950) was applied to a moving window of 100 values to detect and remove outliers. Data gaps smaller than two hours were filled using cubic spline interpolation (similar to Vaughan et al. (2017)). The resulting time series were globally calibrated against the lab measured concentration of NO_3-N (all stations) and against SAC_{254} (all stations but AGR2). Here, probe values averaged one hour before and one hour after sampling were used. EC was calibrated against field values obtained with a handheld WTW probe (WTW Multi 430, Xylem Analytics Germany) for FOR2, while YSI-probes for FOR1, AGR1 and AGR2 were regularly calibrated in field making later corrections obsolete. Parameters of the linear global calibration can be found in Table S3 and indicate a good fit with $R^2 > 0.59$ (mean $R^2 = 0.83$). In a final step, noise in the signal of both discharge and water quality was reduced by a moving average between 2.5 and 6 h (see Table S4). The length of the moving average window was adjusted visually to the variability of the time series and in general larger for the slower reacting larger catchments (see also Rode, Halbedel, et al., 2016).

At the AGR2 station no SAC_{254} lab measurements were available to calibrate the high-frequency SAC_{254} time series. To validate this time series we explored the relationship of SAC_{254} to DOC. At station AGR2 the slope of SAC_{254}-DOC regression is low (Table S1, 0.08 mg m/L) compared to the other catchments (mean 0.18 mg m/L) indicating a potential offset in probe measurements of SAC_{254}. Assuming the SAC_{254}-DOC regression slope (which equals $1/SUVA_{254}$) at AGR2 to be similar to the other stations would result in average SAC_{254} values smaller by a factor of 2 and thus very similar to the neighboring AGR1 catchment. We prefer to leave SAC_{254} at AGR2 uncalibrated noting that C–Q relationships and hysteresis patterns remain unaffected by that.

2.4. Data Analysis

All data analysis was performed using the R statistical software environment and is available as a script in an open repository (Musolff, 2020b).

To test our hypotheses we first detected discharge events using the methodology of Dupas et al. (2016). Details on the manually adjusted parameters can be found in Table S4. The parameters aimed to encompass the full range of discharge in the event to capture the C-Q relationship including the hysteresis. The start of an event was defined in a moving window (5–12 h, Table S4) based on a discharge increase of 10%. The event end was defined when discharge decreased less than 0.3%–0.5% within the moving window. Multiple peaks were considered as one event if discharge dropped less than 50% after discharge peak. Only events above a defined threshold were included (Table S4). Number of separated events ranged from 32 (AGR2) to 56 (AGR1) (Table S4).

After discharge-based event separation, the simple power-law C-Q (Equation 1) as well as the C–Q model accounting for hysteresis (Equation 2) were fitted (minimizing the sum of the square of the errors) separately for each event and constituent. To assess if the addition of the hysteresis parameter is justified, the performance of both models was compared using the Akaike information criterion (AIC). AIC indicate a better performance of Equation 2 when the AIC improvement was larger than two units. We classified the event response from Equation 2 plotting parameter c against parameter b as suggested by Vaughan et al. (2017). To specifically address hypothesis (1) we tested differences of all model parameters across the catchment using the Kruskal-Wallis rank sum test for significance ($\alpha = 0.05$). In case of a significant difference we used the Wilcoxon rank sum test for pairwise comparison with Bonferroni correction for the p-values.

To compare the parameter c from Equation 2 to an established method, we derived the hysteresis index H_I (Lloyd et al., 2016; Vaughan et al., 2017), based on the range-normalized discharge (Q_{norm}) and range-normalized concentration (C_{norm}) of a given event. C_{norm} was linearly interpolated between adjacent measurements at 2% intervals of Q_{norm} to allow comparison for the Q_{norm} intervals that exists on both, rising and falling limb:

$$H_I = \text{mean}\left(C_{\text{norm, rising}} - C_{\text{norm, falling}}\right) \quad (3)$$

Table 2
Statistics on In-Situ Measured Water Quantity and Quality in the Four Catchments

Catchment	Constituent	n	Mean	Median	CV	Min	Max	CV_C/CV_Q	b_{glob}	SE b_{glob}
FOR1	Q [mm/d]	70,080	1.56	0.88	1.28	0.16	27.48			
	EC [µS/cm]	68,680	150.85	148.16	0.12	93.79	310.79	0.10	−0.06	4.1E−04
	NO_3-N [mg/L]	67,447	0.66	0.64	0.33	0.10	2.11	0.26	0.15	1.2E−03
	SAC_{254} [1/m]	66,348	16.27	14.50	0.55	3.73	88.66	0.43	0.11	2.1E−03
FOR2	Q [mm/d]	64,660	0.90	0.45	2.19	0.02	71.12			
	EC [µS/cm]	63,126	191.46	187.78	0.13	126.79	253.61	0.06	−0.09	3.3E−04
	NO_3-N [mg/L]	55,852	0.37	0.36	0.35	0.12	1.29	0.16	0.08	1.3E−03
	SAC_{254} [1/m]	55,895	20.76	18.35	0.61	1.15	73.48	0.28	0.14	2.6E−03
AGR1	Q [mm/d]	62,511	1.12	0.61	1.39	0.05	16.83			
	EC [µS/cm]	68,002	203.07	193.96	0.20	123.16	366.39	0.15	−0.12	4.1E−04
	NO_3-N [mg/L]	64,498	2.60	2.49	0.51	0.20	6.91	0.37	0.36	1.7E−03
	SAC_{254} [1/m]	64,378	21.54	20.29	0.26	11.75	79.92	0.19	0.03	9.1E−04
AGR2	Q [mm/d]	70,080	0.79	0.47	1.26	0.11	12.81			
	EC [µS/cm]	69,872	326.41	321.80	0.19	179.22	484.35	0.15	−0.21	2.8E−04
	NO_3-N [mg/L]	69,430	1.76	1.48	0.65	0.01	4.73	0.51	0.73	1.8E−03
	SAC_{254} [1/m]	65,284	36.36	36.48	0.17	26.26	62.04	0.14	−0.02	7.9E−04

Note. n-Number of Observations, CV-Coefficient of Variation, b_{glob}-Slope of the Inter-annual (Global) logC-logQ relationship. All b_{glob} values are significant ($p < 0.01$). SE b_{glob}-standard error of b_{glob}.

To quantify time lags between concentration and discharge as a potential main control of hysteresis we utilized cross correlation. For the comparison between parameter c, H_I and the time lag Spearman's rank correlation (significance level of $p < 0.01$) was used.

Hypothesis (2) was addressed using two approaches. First, to allow for a discussion on the similarities and differences in event-scale C-Q responses of biogeochemically reactive (NO_3-N and SAC_{254}) and geogenic constituents (represented by EC) we used Spearman's rank correlation between model parameters a, b, and c within each catchments (significance level of $p < 0.01$). Second, to quantify and characterize the role of antecedent conditions for the C-Q response we applied partial least squares regression (PLSR, Wold et al. (2001)), being a robust method that accounts for collinearities among the predicting variables. As predictors we used the 7-, 15- and 30-days mean of the pre-event discharge and water temperature and took event characteristics such as minimum, maximum, cumulative discharge as well as concentration and discharge ranges into account. Similar to Musolff et al. (2015) we used the variable influence on projection (VIP, Wold et al. (2001)) to rank the predictors and the regression coefficient to characterize the direction of influence on the response variable. Only models with $R^2 > 0.5$ are considered and only predictors with a VIP > 1 are reported (Onderka et al., 2012).

3. Results

3.1. Observed Discharge, Concentrations and Inter-Annual C–Q Relationships

Between 56,000 and 70,000 measurements of discharge, EC, NO_3-N and SAC_{254} (equaling 580–730 days) were available for analysis. Here, we report on the basic statistics of the time series (Table 2) and on the inter-annual C-Q relationships from applying Equation 1 to the entire time series.

Mean specific discharge [mm/d] nearly halved from FOR1 to AGR2. This is in line with the decrease in precipitation along the elevation gradient from west to east (Table 1, Figure 2). The variability of discharge was high in all catchments ($CV_Q > 1$) being highest in the small FOR2 catchment ($CV_Q > 2$). Mean EC, in turn, was twice as high in AGR2 compared to FOR1. CV_C/CV_Q clearly indicated chemostatic conditions for EC ($CV_{EC}/CV_Q \leq 0.15$) with an overall dilution C–Q pattern ($b_{glob} < 0$). The strongest dilution pattern coincided

with the highest concentrations in the AGR2 catchment. Among the three constituents standard errors for EC b_{glob} were lowest, indicating only few scatter in the C–Q relationship across all data with decreasing values from FOR1 to AGR2. Note that in the AGR2 catchment, EC was strongly influenced by drainage from an abandoned mine, affecting both the concentration level and the dynamic (Musolff et al., 2015). Concentrations of NO_3-N were consistently low in the more pristine FOR1 and FOR2 catchments (mean ≤ 0.66 mg/L) and high in the more agricultural AGR1 and AGR2 catchments (mean ≥ 1.76 mg/L). CV_C/CV_Q indicates a higher variability in the AGR1 and AGR2 catchments compared to FOR1 and FOR2, with a chemodynamic regime in AGR2 ($CV_C/CV_Q > 0.5$). The global logC-logQ slope b of NO_3-N indicates enrichment patterns ($b_{glob} > 0$) for all catchments with lowest values in FOR2 and highest in AGR2. Standard errors of NO_3-N b_{glob} were higher in the forested compared to the agricultural catchments. Mean SAC_{254} increased from FOR1 to AGR2 by a factor of 2 (see chapter 2.4 on issues in data calibration and validation for station AGR2) while CV_{SAC}/CV_Q clearly decreased. Slope b_{glob} of SAC_{254} was near zero in AGR1 and AGR2 and indicates enrichment patterns in FOR1 and FOR2 ($b_{glob} > 0.10$). Standard errors of b_{glob} for SAC_{254} were higher as for EC and NO_3-N indicating a more scattered C-Q relationship. This was more pronounced for the agricultural than for the forested catchments.

3.2. Storm Event Analysis and Parameter Differences Between Catchments

From the time series of discharge and concentrations events have been separated and event-scale C-Q models have been fitted using Equation 2. In the following separated events are described in terms of number and length. The C-Q model are described in comparison to the simple C-Q models without hysteresis (Equation 1) and in terms of parameter variability between catchments and constituents. Finally, event-scale C-Q model parameters are compared to the inter-annual behavior and to other hysteresis metrics.

The event analyses resulted in a larger number of runoff events in FOR1 ($n = 50$, Table S7), FOR2 ($n = 55$) and AGR1 ($n = 56$) compared to AGR2 ($n = 32$). Events were considerably shorter in the small FOR2 catchments (mean = 1.8 d) compared to the three larger catchments (mean ≥ 3.6 d) covering only 14% of the total time (Table S4). In contrast, in the AGR2 catchment events were longest (mean 6.8 d) and covered 30% of the total time series. The highest number of events with a mean discharge exceeding the 95th percentile of inter-annual discharge was found in FOR2 (25.5% of events) followed by FOR1 (14.0%), AGR2 (9.4%) and AGR1 (8.9%).

The observed continuous time series, global C-Q and selected event models are displayed in Figure 3 and Figures S1–S3. The event-scale C-Q models including the hysteresis parameter (Equation 2) were compared to the models based on the simple power-law model (Equation 1) using the Akaike information criterion (AIC). AIC indicated a better performance (AIC improvement larger than two units) for the models including hysteresis for 538 out of 559 analyzed events (Table S7) thus justifying the addition of a third model parameter. Comparing both models we note that the addition of the hysteresis term to the simple power law formulation left the slope b unaffected (linear regression slope between b from Equations 1 and 2 of 0.99, $R^2 = 0.9$, Figure S4).

The parameters of Equation 2 (see also Figure 1 for interpretation) show distinct differences between constituents, between catchments and over time and allowed for a classification of event responses in terms of b (dilution vs. enrichment) and c (clockwise vs. counterclockwise hysteresis) (overview Figure 4, and in Table S7). The Kruskal-Wallis test confirmed that the distribution of all three model parameters for each constituent significantly differed across the catchments (Table S5). In the following model parameters a, b and c are described separately for each constituent focusing on differences between the catchments.

Parameter a for EC significantly differed between all catchments (pairwise tests, Table S6, Figure 4) and increased from FOR1 over FOR2 to AGR1 and AGR2 (Table S7). The variability of a across all events at each station was however low (CV ≤ 0.13), meaning that concentration levels hardly shifted between events. The majority of events showed dilution patterns for EC with a median $b \leq -0.07$ with significant differences between all catchments except FOR2 and AGR1 (Table S6). The hysteresis parameter c significantly differed between all catchments and indicates a similar proportion of clockwise and counterclockwise events in the catchments FOR1 and FOR2. In contrast, most events showed clockwise hysteresis in AGR1 (84%) and

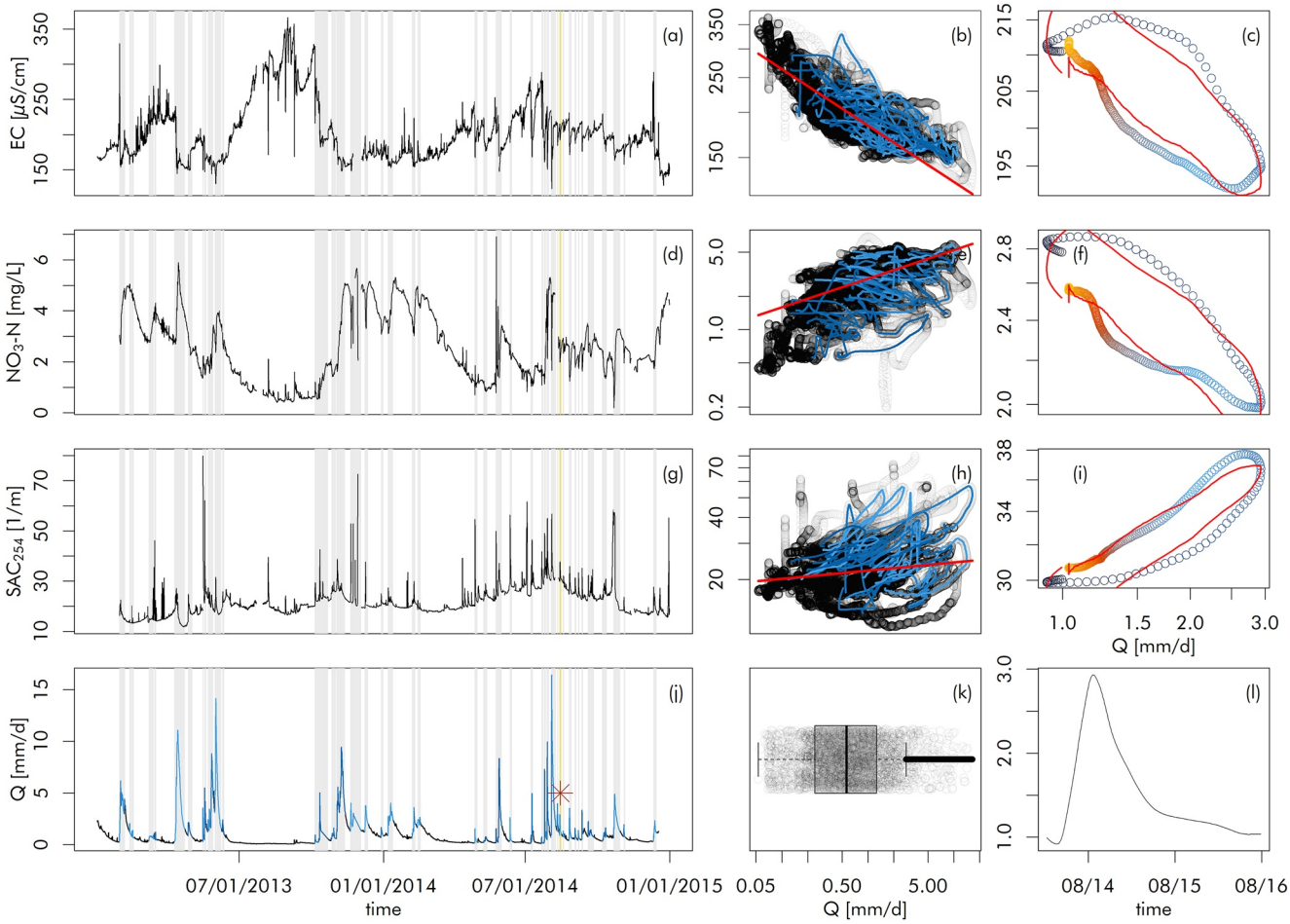

Figure 3. Time series analysis of EC, NO_3-N, and SAC_{254} in the AGR1 catchment. Left column (a, d, g, j) - time series with separated events highlighted with shaded bars; middle column (b, e, h) - global C-Q relationships and power law model (Equation 1); right column (c, f, and i) - example of a modeled event (Equation 2) with observations as dots and the modeled time series as red line; (k) - probability distribution of discharge; (l) time series of the modeled event. Half of the separated events are also plotted as lines in the global C-Q relationships in the second column. The color gradient in the event C-Q plots shows the time from blue at the event start over red to yellow at the event end. The red star in (j) marks the selected event.

counterclockwise hysteresis in AGR2 (84%). Compared to NO_3-N and SAC_{254}, parameters *b* and *c* for EC varied little between events (see scatter in Figure 4d compared to 4h and 4i).

Parameter *a* for NO_3-N significantly differed between all catchments (Table S6). In the agricultural catchments AGR1 and AGR2 parameter *a* was higher and more variable. Catchments FOR1, FOR2 and AGR2 dominantly showed enrichment patterns ($b > 0$) while in AGR1 NO_3-N dilution patterns ($b < 0$) prevailed. Here, parameter *b* did not significantly differed between FOR1 and AGR1 and between FOR2 and AGR2 (Table S6). The hysteresis parameter *c* indicates that counterclockwise events (>70%) dominated for FOR1, FOR2 and AGR2, while more clockwise hysteresis were observed for AGR1 (60%). Here, the pairwise Wilcoxon test revealed no significant differences between most of the catchments (Table S6).

Parameter *a* of the SAC_{254} increased from west to east (FOR1 over FOR2, AGR1 to AGR2) with significant differences between all catchments except FOR2 and AGR1 (Table S6). However, note the explanation on potentially too high SAC_{254} values in AGR2 above. The majority of events in all four catchments showed enrichment patterns for SAC_{254} ($b > 0$). However, the size and variability of *b* consistently decreased from FOR1 to AGR2 (Figure 4j) reflected in significant difference between all catchments except FOR2 and AGR1. Hysteresis parameter *c* was more variable for SAC_{254} compared to EC and NO_3-N (Figures 4d, 4h and 4i). More counterclockwise events were identified for FOR1 and FOR2 (>60%), while a higher number of events with a clockwise hysteresis was found in the AGR1 catchment (>65%). In the AGR2 catchment

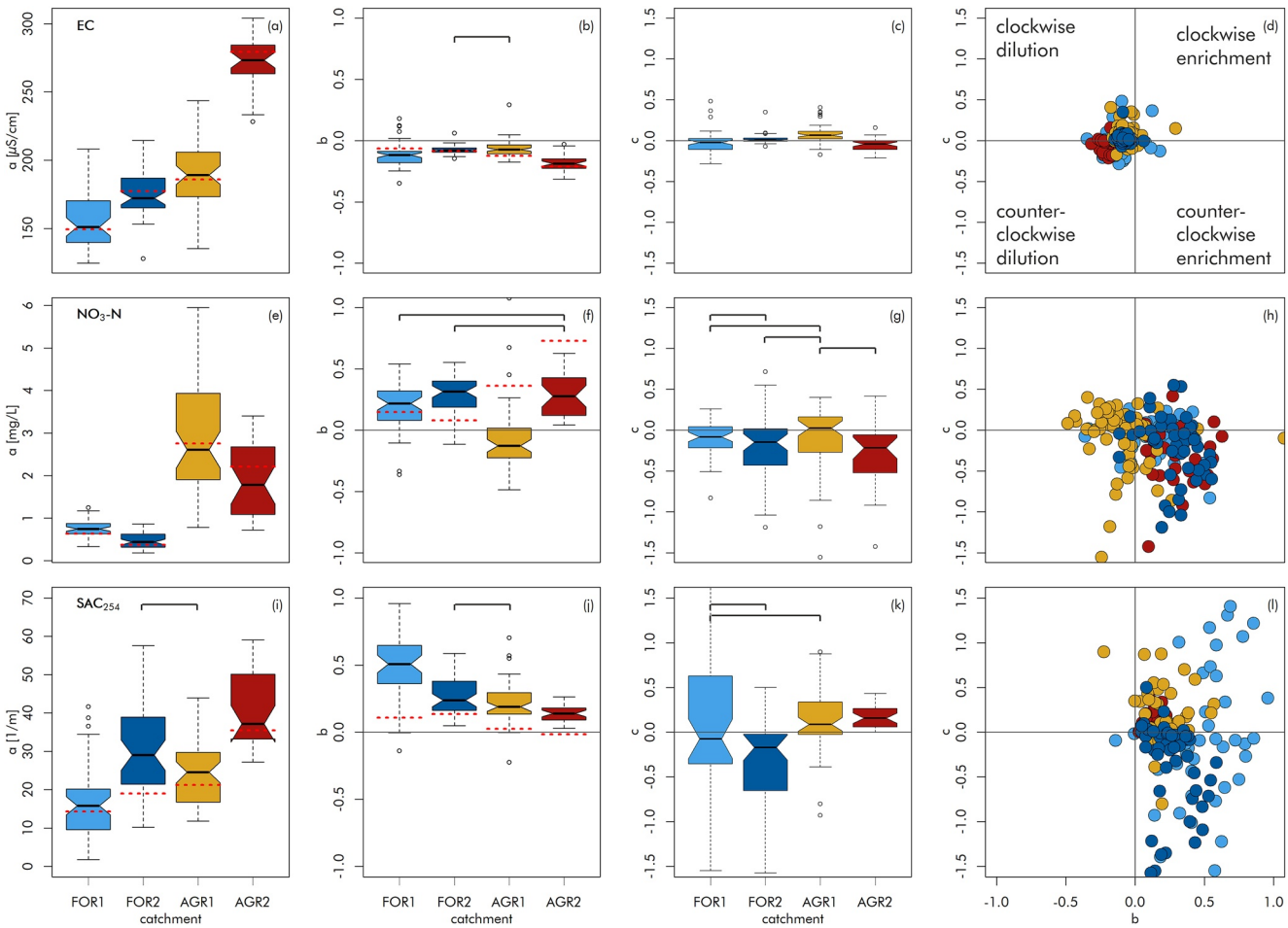

Figure 4. C-Q Hysteresis model parameters *a* (first column), *b* (second column) and *c* (third column) from Equation 2 fitted to the event observations for EC (upper row), NO_3-N (middle row) and SAC_{254} (lower row) separated for each catchment (color scheme of Figure 2). Box plots indicate the parameter variability between events. Parameter *c* was scaled by the global mean concentrations for easier comparison between constituents. Forth column (panels d, h and l) display the C-Q slope *b* against hysteresis indicator *c* for an event classification in a similar way as in Vaughan et al. (2017). Red dashed lines indicate the power law C-Q model parameters a_{glob} and b_{glob} derived across all data. The brackets above the model parameter connect distributions that do not significantly differ ($p > 0.05$, pairwise Wilcoxon rank sum test, see Table S6).

clockwise SAC_{254} hysteresis was detected almost exclusively (>95%). The variability of the parameter *c* between events decreased considerably from FOR1 to AGR2 and the pairwise Wilcoxon test confirmed significant differences between all catchments except for FOR1 with FOR2 and AGR1 (Table S6).

The inter-annual logC-logQ slope b_{glob} using the entire time series was found to be very similar to the median of the slope *b* for the event models for EC and diverging more strongly for NO_3-N and SAC_{254} (Table 2, Figure 4). In the case of NO_3-N in the AGR1 catchment, the global slope b_{glob} indicates an overall enrichment pattern (Figure S2e) while the majority of individual events showed dilution patterns (Figure 4f); in the other catchments the sign of b_{glob} and that of event-scale C-Q slopes were both positive for NO_3-N.

The comparison of model parameter *c* to the established hysteresis index H_I (Lloyd et al., 2016; Vaughan et al., 2017) revealed a good agreement (Figure S5, mean Spearman's rank correlation for all events 0.79). In addition, parameter *c* and the cross-correlation time lag between concentration and discharge in each event was found to be positively correlated (mean rank correlation for all events was 0.68). This relationship only fails for EC in the AGR2 catchment where mine drainage affected EC (Table S7).

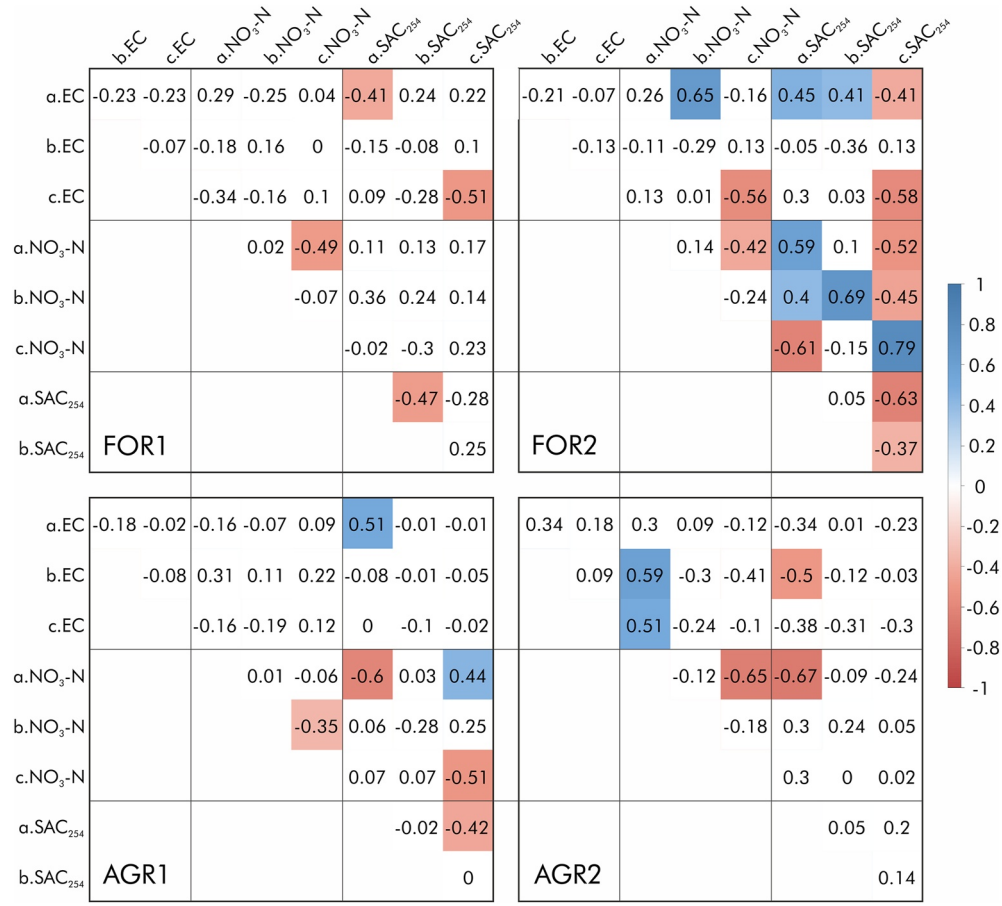

Figure 5. Spearman rank correlation between model parameters for each constituent within each catchment. White tiles are not significant ($p > 0.01$).

3.3. Similarities of Event C-Q Models Across Constituents

The comparison of event parameters *a*, *b* and *c* between constituents within a catchment provides information on similarities and differences in sources and mobilization mechanisms for EC, NO_3-N and SAC_{254} exported by the same events. Overall we found that parameters in the small FOR2 catchment were often strongly positively or negatively correlated with each other. This was not the case for the larger catchments FOR1, AGR1, and AGR2 (Figure 5). In FOR2, rank correlation between NO_3-N and SAC_{254} was highest for the hysteresis parameter *c*, followed by parameter *b* and lowest for *a*. In this catchment, the hysteresis parameter *c* for EC was also negatively correlated with the *c* of NO_3-N and SAC_{254} ($r < 0.55$). In the managed catchments AGR1 and AGR2, parameters *a* for NO_3-N and for SAC_{254} were found to be negatively related to each other ($r < -0.60$).

3.4. C-Q Model Parameter Variability Over Time

The event analysis revealed a variability of model parameters over time in each of the catchments (Figure 4). To explore the role of event- and pre-event conditions on the model parameters of individual events we systematically checked the explorative power of ambient (WT0 - mean event water temperature) and antecedent mean water temperature (WT7, WT15, WT30 - mean water temperature 7, 15, 30 days before the event start) and of ambient (Q0 - mean event discharge, Qmax - maximum event discharge, Qsum - sum of event discharge) and antecedent discharge (Q7, Q15, Q30 - mean discharge 7, 15, 30 days before the event start) using PLSR analysis (Table 3).

Table 3
Partial Least Squares Regression Models to Predict the Model Parameter a, b, and c From Event- And Pre-Event Conditions

	EC			NO_3-N			SAC_{254}								
a	**FOR2**	$R^2 = 0.59$		**AGR2**	$R^2 = 0.83$		**FOR1**	$R^2 = 0.56$		**FOR2**	$R^2 = 0.57$		**AGR2**	$R^2 = 0.72$	
	pred	VIP	dir	Pred	VIP	dir	pred	VIP	dir	pred	VIP	dir	pred	VIP	dir
	WT0	1.40	+	WT0	1.34	-	WT30	1.17	+	WT7	1.48	+	Q30	1.17	-
	WT15	1.35	+	WT30	1.26	-	WT7	1.14	+	WT15	1.44	+	WT7	1.09	+
	WT7	1.34	+	WT7	1.25	-	WT0	1.13	+	WT30	1.42	+	WT30	1.07	+
	WT30	1.26	+	WT15	1.25	-	WT15	1.12	+	WT0	1.29	+	WT0	1.04	+
				Q30	1.11	+	Q0	1.05	-				WT15	1.04	+
							Q30	1.00	-				Q0	1.03	-
b				**FOR2**	$R^2 = 0.52$	dir	**FOR2**	$R^2 = 0.56$	dir						
				pred	VIP		pred	VIP							
				WT7	1.29	+	Q30	1.40	+						
				WT15	1.28	+	Qmax	1.30	-						
				WT0	1.25	+	Qsum	1.30	-						
				WT30	1.21	+	Q0	1.19	-						
				Q0	1.09	-									
c	**FOR2**	$R^2 = 0.55$	dir				**FOR2**	$R^2 = 0.60$	dir	**AGR2**	$R^2 = 0.51$	dir			
	pred	VIP					pred	VIP		pred	VIP				
	Qmax	2.00	+				WT0	1.31	-	Qmax	1.59	+			
	Q0	1.32	-				WT15	1.09	+	Qsum	1.49	+			
	Qsum	1.27	-				WT30	1.07	+	Q0	1.30	+			
							WT7	1.07	-	Q7	1.04	-			
							Qmax	1.06	-						
							Q0	1.00	+						

Note. Only models with $R^2 > 0.5$ are reported. Models are separated by constituent, catchment, and the three predicted model parameters. For each model the most relevant predictors (pred) are ranked by the VIP value. Only predictors with a VIP > are reported. dir - direction of influence of the predictors derived from the PLSR model coefficients. A full correlation matrix of model parameters with the predictors in all catchments is given in Figure S6.

The PLSR analysis yielded 10 out of 26 models with $R^2 > 0.5$. Most of those regression models satisfactorily predict event model parameters for SAC_{254} ($n = 6$) while only two models predict parameters for EC and NO_3-N with acceptable performances.

PLSR models for EC were found acceptable for the small FOR2 catchment only. Here parameter *a* was well predicted by event- and antecedent water temperature indicating higher EC values with higher water temperature. Parameter *c* was predicted by event discharge metrics. Higher maximum discharge within an event was connected to a more pronounced clockwise hysteresis while mean event discharge and sum of event discharge had an opposite effect on parameter *c*.

The regression analysis for NO_3-N showed that parameter *a* in AGR2 was controlled by event- and antecedent water temperature and discharge yielding the highest R^2 of all PLSR models. Parameter *a* in AGR2 thus shows a clear seasonal pattern with increasing values and consequent shifts of C-Q event relationships with colder and wetter conditions. The rank correlation analysis indicated a similar relationship for AGR1 (Figure S6) not strong enough, however, for an acceptable PLSR model. The temporal changes of parameter *b* of NO_3-N in FOR2 were predicted mainly by antecedent and event water temperature indicating steeper C-Q slopes under warmer conditions.

The PLSR analysis for SAC_{254} yielded similar models satisfactorily predicting parameter *a* in the forested catchments FOR1 and FOR2 mainly from antecedent and event water temperature. In AGR2 a high parameter *a* was linked to low antecedent discharge 30 days before the event and to high water temperatures

as well. Consequently SAC_{254} levels of the analyzed events are characterized by a pronounced seasonality with high values under dry and warm conditions across the forested catchments and AGR2. The inter-event variability of parameter *b* in FOR2 was linked to antecedent and event discharge conditions. Here, wetter antecedent conditions and smaller events (low maximum, mean and sum of event discharge) were connected to steeper event-scale C–Q relationships. Hysteresis parameter *c* in FOR2 was mainly explained by water temperature but with mixed directions. A more pronounced (wider) counterclockwise hysteresis pattern was connected to colder event temperatures but warmer antecedent conditions. In AGR2 parameter *c* varied mainly with event discharge indicating more pronounced clockwise hysteresis with larger events.

4. Discussion

4.1. Controls of C-Q Relationships at the Event Scale

The exploration of model parameters fitted for each event (Equation 2) allows an interpretation on the location of solute mobilization in the catchment and changes in source with time. Our analysis considers solutes with geogenic, biogenic and anthropogenic sources in both agriculturally managed and more pristine forested catchments. The following sections addresses hypothesis (1) on the land use control on event-scale C-Q relationships by discussing the findings for EC across all catchments and the findings for NO_3-N and SAC_{254} separated by the forested and agricultural catchments.

4.1.1. Similarity of EC Dynamics Across all Catchments

Specific conductance EC is a sum parameter of dissolved ions and therefore depends on the major ion concentrations. In the studied catchments these include calcium, sulphate, magnesium and chloride (Musolff et al., 2015) with a dominant geogenic origin. The groundwater dominated base flow has the highest concentrations of these solutes and is likely increasingly diluted with an increase of younger and shallower water components during discharge events. The dependence of geogenic major ions and thus EC in the stream on the depth of the source similar to the transit time since ion mobilization has been demonstrated before using modeling and data-driven approaches (Botter et al., 2020; Musolff et al., 2017a; Zhi et al., 2019). This is reflected in the mildly negative slope *b* for EC across FOR1, FOR2 and AGR1 (Table 2, Figure 3) catchments which has also been observed for geogenic solutes across a wide range of catchments (Godsey et al., 2009; Knapp et al., 2020; Rose et al., 2018). The export regime of EC (CV_C/CV_Q, Table 2) was overall chemostatic with only minor concentration variability compared to discharge variability (Table 2). At the event scale, C-Q parameters varied little between events which underlines the spatial and temporal stability of the mobilization mechanism described above (Figure 4). Among the four catchments, median concentrations and model parameter *a* systematically decreased as annual runoff increased (Figure 4). This strong hydroclimatic control on average concentrations of geogenic solutes is in line with the findings of Godsey et al. (2019) along a much wider range of different catchments. In the small FOR2 catchment the high predictive power of water temperature on parameter *a* (PLSR in Table 3) can be interpreted as a temperature effect on weathering and thus availability of geogenic solutes, similar to findings of Knapp et al. (2020) for magnesium. This effect seems not to be evident in the larger catchments FOR1, AGR1 and AGR2. Hysteresis loops were of minor importance for the C-Q relationship of EC (Figure 4). Among the different catchments with contrasting land use (excluding mine drainage in AGR2), differences in both parameters *b* and *c* of EC were small compared to those for NO_3-N and SAC_{254} (Figure 4). This similarity across all catchments hint to a similar source in groundwater and a similar mobilization mechanism as described above that is independent from land use and hydroclimatic settings. This is further justified by the similarity in the geological settings and the major ion chemistry (Musolff et al., 2015). Our starting hypothesis (1) on the land-use control of source arrangement and C-Q relationships does thus not hold true for EC and the group of geogenic solutes with a low reactivity.

4.1.2. Coupled NO_3-N and SAC_{254} Event Behavior in Forested Catchments

In contrast to EC the C-Q behavior of NO_3-N as well as SAC_{254} was clearly different between the forested and agriculturally managed catchments corroborating hypothesis (1). Concentration of NO_3-N was generally low in the forested catchments and the event-scale analysis revealed a dominance of counterclockwise enrichment patterns (Figure 4), indicating a delayed increase in concentration compared to discharge. Parameter *a* varied between events and exhibited a seasonal trend, as reflected in the high predictive power

of water temperature and antecedent discharge (FOR2) (Table 3) comparable to the findings of Knapp et al. (2020). In agreement with other studies in forested settings (Duncan et al., 2017; Knorr, 2013; Koenig et al., 2017), we found mainly NO_3-N enrichment C–Q patterns. However, the same studies reported mainly clockwise hysteresis, while we found for >69% counterclockwise hysteretic patterns. Knorr (2013), Koenig et al. (2017) and Duncan et al. (2017) argue for a finite pool of NO_3-N in the riparian zone and shallow groundwater that is exhausted during the events which seems not to be the case in our catchments.

Although positive C-Q patterns at the event scale prevailed for SAC_{254}, we observed a clear difference of event behavior between forested and agricultural catchments. In the forested catchments C-Q slopes (*b*) were more strongly positive, while parameter *a* was lower and hysteresis parameter *c* showed a higher variability over time (Figure 4) with a high share of events revealing counterclockwise hysteresis. The counterclockwise hysteresis is in line with findings of Strohmeier et al. (2013) and Vaughan et al. (2017) for DOC in forested catchments. Both argue for a greater connectivity of near stream riparian wetland DOC source zones on the falling limb of the event hydrograph. This also agrees with a model-based assessment by Zhi et al. (2019) stating that the hysteresis links to higher rates in the reaction providing DOC from soil organic matter in the uppermost part of the soil. The generally positive (parameter *b*) C-Q response in catchments with well-connected wetlands corresponds with findings of Winterdahl et al. (2014), Musolff et al. (2018), and Zarnetske et al. (2018), with analyses over a large range of catchments. The reason for this enrichment patterns were shown to be the higher availability of DOC in the shallow organic soil horizons in contrast to low DOC availability in deeper groundwater. The soil sources get increasingly activated when the catchment wets up and near-surface flow paths are activated as demonstrated by both modeling and data-driven approaches (Musolff et al., 2018; Richardson et al., 2020; Seibert et al., 2009; Zhi et al., 2019). At the small FOR2 catchment we found a strongly positive correlation between NO_3-N and SAC_{254} hysteresis parameters *c*, but also between C-Q slope *b* and parameter *a* (Figure 5) pointing to a similar source of both constituents. Werner et al. (2019) could link the DOC concentration and quality dynamics in FOR2 to the hydroclimatically controlled biogeochemical conditions in the riparian zone. In the data presented here, this is reflected in the predictive power of antecedent conditions for the model parameters at the forested sites (Table 3). Warm antecedent conditions are connected to a faster decomposition of soil organic matter, a higher availability of DOC and thus SAC_{254} as well as NO_3-N in the permanently wet riparian source zone (Zhi et al., 2019) resulting in higher concentrations (parameter *a*), steeper C-Q slopes (*b*) and more pronounced hysteresis (*c*). In the riparian zone, nitrification and denitrification can lead to a very close spatial (vertical) proximity of nitrate and DOC source zones (Frei et al., 2012; Riedel et al., 2013). This suggests that in the studied forested catchments dominant sources for the stream export SAC_{254} and NO_3-N can be found in the top-soil horizons of the riparian zones reflected in the tight positive correlation of event-scale C-Q parameters in FOR2. This coupling was not as clear for the larger FOR1 catchment (Figure 5) and possibly blurred by the overall higher variability of C-Q parameters between events.

4.1.3. Agricultural Management Defines NO_3-N Event Behavior

The agricultural catchments are characterized by much higher NO_3-N concentration compared to the forested catchments (Table 2, Figure 4). At the event-scale we found difference between AGR1 with more clockwise dilution and AGR2 with more counterclockwise enrichment NO_3-N event C-Q patterns while the seasonal temporal variation in concentration is comparable (Figure 4). The event behavior in AGR1 is similar to NO_3-N event analysis in agricultural catchments by Fovet et al. (2018), Lloyd et al. (2016) and Rose et al. (2018). The observation of a positive global C-Q pattern across all data but a dilution at the event scale was described by Dupas et al. (2016) and also for 24% of 219 French catchment studied by Minaudo et al. (2019). The observed event-scale C-Q behavior of NO_3-N in the AGR1 catchment mimics geogenic solutes with a higher availability in deeper groundwater compared to shallower event water (Seibert et al., 2009) and a lower concentration at the falling limb of the hydrograph. In contrast the AGR2 catchment behaved very consistently across events with regards to C-Q slope *b* and hysteresis parameter *c* (Figure 4). Slope *b* was indicating enrichment patterns and was similar between event- and global C-Q response. This is in line with findings of Yang et al. (2018) in a subcatchment of the AGR2 and Musolff et al. (2016) who showed that higher water levels lead to a stronger connectivity between the stream and the shallow young, NO_3-N rich groundwater. It was suggested that tile drains exaggerate this relationship (Musolff et al., 2015). Interestingly there is a similarity of NO_3-N C-Q pattern (parameter *b* and *c*) in the AGR2 catchment with the forested catchments (Figure 4) but at a much higher concentration level. This similarity

between agricultural and undeveloped sites was also stated by (Zhi & Li, 2020). The more effective drainage of the NO_3-N source on the falling limb of the hydrograph in the riparian soils of the forested catchments seems to be functional similar to the role of tile drainage in the agricultural catchment. Consequently, we need to refine the starting hypothesis (1): Different land use patterns can lead to similar C-Q patterns at the event scale when source arrangement and mobilization mechanisms work in a comparable way.

The dominance of counterclockwise patterns with higher concentrations on the falling limb of the hydrograph is in line with findings of Outram et al. (2016) where it is shown that tile drains create these hysteretic patterns and stated by (Zhang et al., 2020) as well. The AGR2 catchment also exhibits a high predictive power of water temperature and antecedent discharge on model intercept *a* (Table 3). This stresses the role of NO_3-N source zone availability in the cold season without plant uptake and of catchment wetness in shaping the connectivity between NO_3-N source zone and the stream. The question remains why two neighboring catchments with comparable land use, geology, topography and climatic characteristics exhibit diverging C-Q slopes and hysteresis at the event scale. We hypothesize that this can be related to agricultural management in the near stream zones. The AGR1 catchment drains into a drinking water reservoir which means that in a 100 m zone around the stream, the use of fertilizer is not allowed and inputs from tile drains are strongly regulated. In consequence near the stream the NO_3-N abundance is higher in the deeper groundwater fed from the agricultural hinterland compared to shallow ground- and soil water. We thus argue that the AGR1 catchment does not have a pronounced shallow near stream source zones of NO_3-N (absence of fertilization) and nor efficient connectivity of hinterland NO_3-N sources (absence of tile drains) exists. The lack of wide buffer zones with restricted fertilization in AGR2 lead to a high abundance of NO_3-N in shallow ground- and soil water while denitrification was shown to partly remove NO_3-N in deeper and older groundwater components in this catchment (Nguyen et al., 2021; Yang et al., 2018). The interplay of source distribution with the efficient connectivity by tile drains (Musolff et al., 2015) can explain the observed homogeneous positive event C-Q slopes and dominance of counterclockwise hysteresis in the AGR2 catchment. However, to fully disentangle the effect of spatial source heterogeneity in conjunction with potential differences in the spatial pattern of rainfall and discharge generation a spatially distributed monitoring and modelling approach in both agricultural catchments would be needed.

In both agriculturally managed catchments the event C-Q responses of SAC_{254} were higher in model intercept *a* but weaker and positive in *b* and less variable in both *b* and *c*. Here, clockwise C-Q patterns prevailed (Figure 4). Model parameter *a* of SAC_{254} was inversely related to parameter *a* of NO_3-N for the same events (Figure 5) and exhibited a clear seasonality with positive predictive power of water temperature in AGR2 (Table 3). The inverse carbon-NO_3-N concentration relationship was described for larger scale datasets (Ebeling et al., 2021; Guillemot et al., 2021) and across different ecosystems globally (Taylor and Townsend, 2010). This is also in line with a better mobilization of DOC under NO_3-N reducing conditions in riparian zones (Musolff et al., 2017b; Strohmenger et al., 2020). The lower SAC_{254} on the falling limb of the hydrograph that creates clockwise hysteresis also reflects lower DOC concentrations in the shallow NO_3-N source zones as discussed by Fovet et al. (2018). Fast connectivity of NO_3-N rich and DOC depleted source zones by tile drains may further enhance this tight coupling. Overall SAC_{254} behavior shows that the near-stream source of DOC is likely similar in all catchments and therefore less controlled by land use and more by topographical settings and soil type distribution. However, biogeochemically mediated availability of DOC and hydrological connectivity can differ between catchments with similar sources.

4.2. How Do Event-Scale and Inter-Annual C-Q Models Align?

With regards to hypothesis (2) we found discrepancies between global and event-scale models that differed between solutes and catchments (Figure 6). In consequence, the event analysis added insights into solute mobilization in some but not in all cases. It is worth noting that for the AGR1 and AGR2 catchment a previous study provides an analysis of long-term slope *b* for EC, NO_3-N and total organic carbon, (biweekly to monthly data from 1993–2009, Musolff et al. (2015)) that is nearly identical to the two-year b_{glob} (2013–2014) reported here. This hints to a robustness of the C-Q slope b_{glob} also for shorter time periods as well as to a persistence of C-Q relationships in time.

We found a close similarity of the inter-annual logC-logQ slope b_{glob} of the entire EC time series to the event scale parameter *b* (Figure 6 upper row). Since the event model parameters *a*, *b* and *c* did not vary

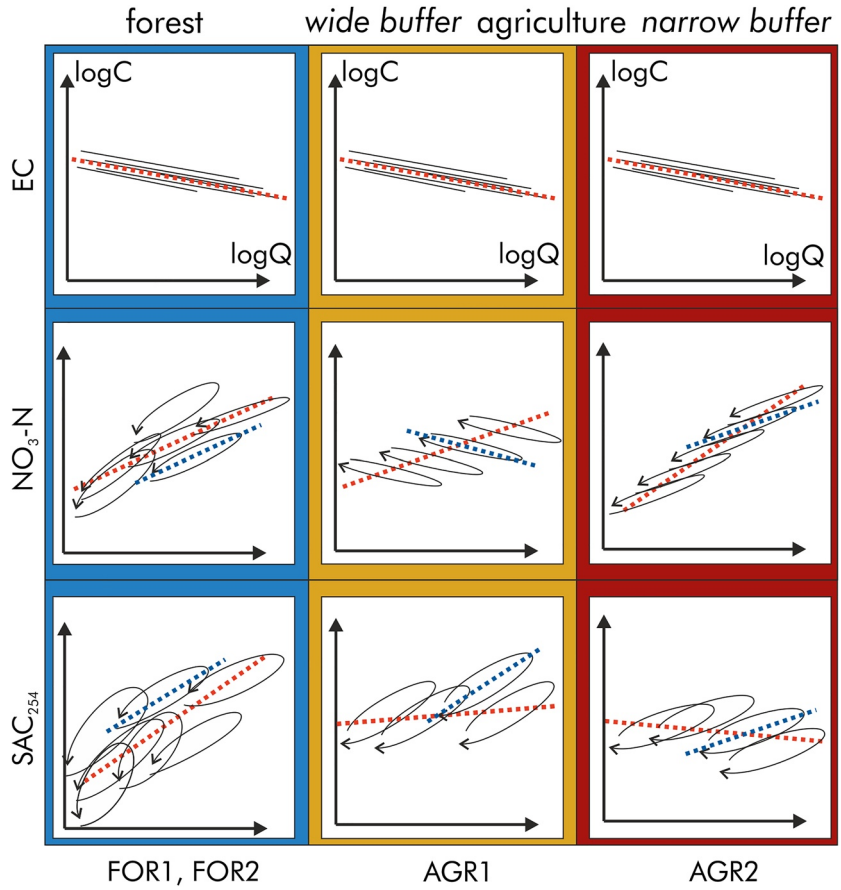

Figure 6. Composite logC-logQ plots combining individual event responses of different constituents over time in forested and agricultural catchments. Agricultural catchments are separated based on their management practice (protected wide vs. narrow non protected buffer zones). The blue solid lines show event-scale C-Q slope. The red dashed lines represent the global C-Q relationship across the entire time series. The arrows indicate the direction of the hysteresis. Background colors refer to the catchments in Figure 2.

considerably between the events, the resulting global power law C-Q relationship was robust and allowed us to draw similar conclusions on sources and mobilization mechanisms following the idea of higher concentrations in older and deeper groundwater compared to shallower and younger soil water as described in chapter 4.1. The added value of event-scale analysis compared to inter-annual C-Q analysis is therefore rather minor when assessing geogenic solutes with low reactivity or EC.

In the forested catchments we found a general agreement of parameter b_{glob} for NO_3-N and SAC_{254} with the event scale C-Q patterns leading to similar conclusions on proximal (shallow), hydrologically connected sources for both constituents (Figure 6, middle row). A considerable variability in the event model parameters *b* and *c* point to a large scatter in the global C-Q relationship. That is a clear indication of variable hydrological or biogeochemical conditions before and during the different events that control availability of NO_3-N and DOC as hypothesized and as discussed in detail in chapter 4.1 above. In consequence, the analysis of the variability between events clearly adds insight into the role of antecedent conditions on SAC_{254} or NO_3-N mobilization and exports that cannot be captured in inter-annual C-Q models.

In the agricultural catchment AGR1 global and event-scale C-Q patterns for NO_3-N diverged, clearly indicating the added value of event-scale analysis for understanding the role of protected stream buffer zones on NO_3-N mobilization. This behavior resembles Simpson's paradox (Simpson's reversal) a statistical phenomenon of diverging trends within and across groups (Simpson, 1951). For the C-Q relationship of NO_3-N in AGR1 the means that we cannot determine the global C-Q response from responses at the event scale. An interpretations of the C-Q relationship with coarser temporal resolution may therefore lead to a false or

incomplete inference of the underlying processes. In contrast, in the agricultural catchment AGR2 without a protected buffer zone the global C-Q relationship was aligned with the event-scale patterns that only showed low variability in the model parameter *b* and *c* between events. This was also observed by Knapp et al. (2020) and by Rose et al. (2018) for EC and geogenic solutes such as magnesium, calcium and sodium. For NO_3-N this similarity in behavior hints to a homogeneity of event responses in intensively managed agricultural catchments as also stated by Thompson et al. (2011), Basu et al. (2010) and by Rose et al. (2018). The reasoning behind that lies in the strong NO_3-N source from fertilizers in the agricultural catchments, as well as the enhanced connectivity of source zones and stream by tile drains in the AGR2 catchment (Dupas et al., 2017; Musolff et al., 2015). This catchment can be seen as an archetype of a managed catchment where NO_3-N export is similar across events and dominantly controlled by hydrologically induced connectivity of NO_3-N source and the stream network. We also note that this functional homogeneity of hydrologically driven exports is not necessarily connected to chemostatic export regimes. Consequently we need to refine hypothesis (2): Biogeochemically reactive solutes do not necessarily exhibit contrasting C-Q relationships at event- and inter-annual scale when intensive agriculture homogenize sources and mobilization mechanisms.

In the agricultural catchments, the global C-Q behavior of SAC_{254} was hardly captured by the single inter-annual power law model. The generally positive event-scale C-Q patterns shift in their level (parameter *a*) with antecedent discharge conditions to stack to a non-identifiable global C-Q pattern (see the discussion on Simpson's paradox above) independent of the presence of protected buffers (Figure 6). Here the event analysis allowed for insights into mobilization processes driven by the interplay of biogeochemical and hydrological processes as hypothesized and as described in chapter 4.1 that would not be obtained with inter-annual low-frequency C-Q analysis.

Large scatter and high standard errors of parameter *b* in inter-annual C-Q relationships can be an indicator for a divergence of event-scale behavior. In that case a careful evaluation is needed that may separate event from non-event samples (see e.g., Minaudo et al. (2019)) to not draw wrong conclusions on solute sources and mobilization mechanisms.

In general, we found that the variability of the event scale C-Q model parameters for the small FOR2 catchment were more often explainable by event- and antecedent conditions than for the other, larger, catchments (Table 3). This was especially true for the hysteresis parameter *c* that was predictable for two of the three studied constituents in FOR2 but only for one constituent in all other catchments. We argue that this parameter is particularly sensitive to small variations in event timing and catchment heterogeneity while parameters *a* and *b* are more robust and stable across events. In a small headwater catchment a rainfall event will lead to a more homogeneous and synchronous discharge and solute mobilization response. Large catchments will exhibit stronger differences in discharge timing in different parts of the catchment when a rainfall event passes through. Hysteresis is especially sensitive to discharge and solute mobilization timing because short time shifts between both can lead to large hysteresis (see Table S7, mean time shifts between C and Q for NO_3-N and SAC_{254} are smaller than one hour). In the integration at the catchment outlet this may lead to less traceable hysteretic patterns as also described by Vaughan et al. (2017) and by Butturini et al. (2008). This may be especially true in catchments with heterogeneous solute sources. Classifying the type of rainfall event and the discharge response in a better way (e.g., Tarasova et al. (2018)), may help resolving differences between event C-Q responses.

5. Conclusions and Outlook

In this study we analyze two-year time series of specific conductance, nitrate and spectral absorbance as a surrogate for dissolved organic carbon in four neighboring catchments by applying a model that captures concentration level (parameter *a*), C-Q slope (*b*) and hysteresis (*c*) at the same time. The model parameter *c* describes direction and magnitude of hysteresis and compared well to the established hysteresis index. The model used here does not aim to replace the established index but rather to provide an alternative straightforward approach when the integration of event- and inter-annual C-Q patterns are of interest.

The study catchments represent a hydroclimatic gradient and range from more pristine forested to agriculturally managed conditions. As hypothesized, we found a land use control on the event-scale C–Q behavior

and differences between geogenic and biogeochemically reactive solutes in terms of inter-event variability. However we need to refine our initial hypothesis as solute-specific differences can occur. We found that EC dynamics were well captured by a global C–Q analysis derived from inter-annual time series. The C–Q slope hardly changed between the events and hysteresis was not pronounced. The dilution behavior with chemostatic export regimes (low CV_C/CV_Q ratio) was consistent between catchments, independent of land use and resembled the typical pattern of hydrologically controlled geogenic solutes. In contrast, SAC_{254} was strongly variable between events with dominantly positive C-Q patterns and more pronounced hysteresis as a result of the interplay of biogeochemical controlled availability of DOC in near stream riparian soils and hydrologically controlled exports. An inter-annual C–Q analysis across all events was able to capture the general positive C–Q pattern but not the strong variability between events. In contrast there was less variability between events for the agricultural catchments but individual positive C–Q relationships at the event scale stack to an unclear inter-annual C–Q relationship that does not allow any inference of underlying processes. NO_3-N also responded differently in forested and agricultural catchments. In the forested catchments we observed a similarity of NO_3-N and SAC_{254} exports at the event scale that points to similar sources and export mechanisms. In one of the agricultural catchments we found a functional homogeneity of NO_3-N event responses with steep positive C–Q slopes that is reflected in the similarity of event-scale and global-scale C–Q analysis. Here, exports were dominantly controlled by connectivity to the agricultural source zones. In contrast, event behavior was different in the agricultural catchment that drains into a drinking water reservoir. A more strict regulation of near-stream zones in terms of fertilizer application and the absence of tile drains may explain the negative event-scale C–Q slopes while the overall concentration level was found to be comparable to the other managed catchment.

In consequence, event-scale C–Q analysis provided more insights when the global composite C-Q relationship was not able to capture the dynamic concentration behavior especially true for biogeochemically reactive solutes. We also found that the hysteretic behavior of concentrations were most consistent in the small headwater catchment. Here, we could better predict the magnitude and direction of hysteresis parameter *c* from antecedent and event conditions. In larger catchments, however, we found the hysteresis to be less traceable. We argue that the hysteresis is very sensitive to different timing and mixing of storm events in larger catchments. This may blur the mechanistic meaning of the hysteresis. We also note that the logC-logQ slope *b* is more robust against this mixing. In conclusion, the interpretation of hysteresis should be handled with care and is likely most helpful in headwater catchments.

We hope analyzing the growing availability of high-frequency data across a larger range of catchment properties will provide more insights into mechanisms of reactive solute transport at the catchment scale in the future. Here, a refinement of the typology of a storm event that can be extracted from rainfall and discharge patterns is a promising approach (Tarasova et al., 2018). Adding more advanced measures of concentration and discharge variability such as spectral analysis (Hensley et al., 2018) or using machine-learning techniques (Aguilera & Melack, 2018) will furthermore improve our understanding of catchment-scale transport processes. In turn we argue that a better understanding gained from event-scale behavior of high-frequency data will feed back into the interpretation of low-frequency C-Q analysis especially with diverging global or seasonal versus event-scale C-Q patterns as shown by Minaudo et al. (2019).

Data Availability Statement

For this research are available in these in-text data citation references: Musolff (2020a) [creative commons attribution CC BY], LHW (2018) [for scientific, non-commercial use only], Cornes et al. (2018) [observational data are strictly for use in non-commercial research and non-commercial education projects only], EEA (2013) [no limitations on public access], (CLC, 2016) [no limitations on public access].

Acknowledgments
The research was supported by TERENO (TERrestrial ENvironmental Observatories) funded by the Helmholtz Association and the Federal Ministry of Education and Research (BMBF). The authors would like to thank the technical staff at UFZ without whom this research would not have been possible: Uwe Kiwel, Burkhardt Kühn and Toralf Keller. Moreover we thank Marieke Osterwoud and Xiangzhen Kong for sharing their datasets with us. We also thank the reviewers and editors for their positive comments that helped improving the manuscript. We acknowledge the E-OBS data set from the EU-FP6 project UERRA (http://www.uerra.eu) and the data providers in the ECA&D project (https://www.ecad.eu). Qing Zhan was funded by a master scholarship Otto-von-Guericke by Magdeburg-Stendal University of Applied Sciences and the city of Magdeburg, Germany during this study. Open access funding enabled and organized by Projekt DEAL.

References

Aguilera, R., & Melack, J. M. (2018). Concentration-discharge responses to storm events in Coastal California Watersheds. *Water Resources Research*, *54*(1), 407–424. https://doi.org/10.1002/2017wr021578

Ameli, A. A., Beven, K., Erlandsson, M., Creed, I. F., McDonnell, J. J., & Bishop, K. (2017). Primary weathering rates, water transit times, and concentration-discharge relations: A theoretical analysis for the critical zone. *Water Resources Research*, *53*, 942–960. https://doi.org/10.1002/2016WR019448

Bao, C., Li, L., Shi, Y. N., & Duffy, C. (2017). Understanding watershed hydrogeochemistry: 1. Development of RT-Flux-PIHM. *Water Resources Research*, *53*(3), 2328–2345. https://doi.org/10.1002/2016wr018934

Basu, N. B., Destouni, G., Jawitz, J. W., Thompson, S. E., Loukinova, N. V., Darra–, A., et al. (2010). Nutrient loads exported from managed catchments reveal emergent biogeochemical stationarity. *Geophysical Research Letters*, *37*, L23404. https://doi.org/10.1029/2010gl045168

Basu, N. B., Thompson, S. E., & Rao, P. S. C. (2011). Hydrologic and biogeochemical functioning of intensively managed catchments: A synthesis of top-down analyses. *Water Resources Research*, *47*, W00J15. https://doi.org/10.1029/2011wr010800

Bieroza, M. Z., & Heathwaite, A. L. (2015). Seasonal variation in phosphorus concentration-discharge hysteresis inferred from high-frequency in situ monitoring. *Journal of Hydrology*, *524*, 333–347. https://doi.org/10.1016/j.jhydrol.2015.02.036

Birkel, C., Broder, T., & Biester, H. (2017). Nonlinear and threshold-dominated runoff generation controls DOC export in a small peat catchment. *Journal of Geophysical Research: Biogeosciences*, *122*(3), 498–513. https://doi.org/10.1002/2016JG003621

Blaen, P. J., Khamis, K., Lloyd, C., Comer-Warner, S., Ciocca, F., Thomas, R. M., et al. (2017). High-frequency monitoring of catchment nutrient exports reveals highly variable storm event responses and dynamic source zone activation. *Journal of Geophysical Research: Biogeosciences*, *122*(9), 2265–2281. https://doi.org/10.1002/2017jg003904

Boland-Brien, S. J., Basu, N. B., & Schilling, K. E. (2014). Homogenization of spatial patterns of hydrologic response in artificially drained agricultural catchments. *Hydrological Processes*, *28*(19), 5010–5020. https://doi.org/10.1002/hyp.9967

Botter, M., Li, L., Hartmann, J., Burlando, P., & Fatichi, S. (2020). Depth of solute generation is a dominant control on concentration-discharge relations. *Water Resources Research*, *56*(8), e2019WR026695. https://doi.org/10.1029/2019WR026695

Burns, D. A., Pellerin, B. A., Miller, M. P., Capel, P. D., Tesoriero, A. J., & Duncan, J. M. (2019). Monitoring the riverine pulse: Applying high-frequency nitrate data to advance integrative understanding of biogeochemical and hydrological processes. *Wiley Interdisciplinary Reviews-Water*, *6*(4), e1348. https://doi.org/10.1002/wat2.1348

Butturini, A., Alvarez, M., Bernal, S., Vazquez, E., & Sabater, F. (2008). Diversity and temporal sequences of forms of DOC and NO3-discharge responses in an intermittent stream: Predictable or random succession? *Journal of Geophysical Research: Biogeosciences*, *113*(G3), G03016. https://doi.org/10.1029/2008jg000721

Carpenter, S. R., Stanley, E. H., & Vander Zanden, M. J. (2011). State of the World's freshwater ecosystems: Physical, chemical, and biological changes. *Annual Review of Environment and Resources*, *36*, 75–99. https://doi.org/10.1146/annurev-environ-021810-094524

CLC. (2016). *CORINE land cover 2012 v18.5*. Retrieved from https://land.copernicus.eu/pan-european/corine-land-cover

Cornes, R. C., van der Schrier, G., van den Besselaar, E. J. M., & Jones, P. D. (2018). An ensemble version of the E-OBS temperature and precipitation data sets. *Journal of Geophysical Research-: Atmospheres*, *123*(17), 9391–9409. https://doi.org/10.1029/2017jd028200

Duncan, J. M., Band, L. E., & Groffman, P. M. (2017). Variable nitrate concentration-discharge relationships in a forested watershed. *Hydrological Processes*, *31*(9), 1817–1824. https://doi.org/10.1002/hyp.11136

Dupas, R., Abbott, B. W., Minaudo, C., & Fovet, O. (2019). Distribution of landscape units within catchments influences nutrient export dynamics. *Frontiers in Environmental Science*, *7*.ARTN 43. https://doi.org/10.3389/fenvs.2019.00043

Dupas, R., Gruau, G., Gu, S., Humbert, G., Jaffrezic, A., & Gascuel-Odoux, C. (2015). Groundwater control of biogeochemical processes causing phosphorus release from riparian wetlands. *Water Research*, *84*, 307–314. https://doi.org/10.1016/j.watres.2015.07.048

Dupas, R., Jomaa, S., Musolff, A., Borchardt, D., & Rode, M. (2016). Disentangling the influence of hydroclimatic patterns and agricultural management on river nitrate dynamics from sub-hourly to decadal time scales. *The Science of the Total Environment*, *571*, 791–800. https://doi.org/10.1016/j.scitotenv.2016.07.053

Dupas, R., Musolff, A., Jawitz, J., Rao, P. S. C., Jager, C. G., Fleckenstein, J. H., et al. (2017). Carbon and nutrient export regimes from headwater catchments to downstream reaches. *Biogeosciences*, *14*(18), 4391–4407. https://doi.org/10.5194/bg-14-4391-2017

Ebeling, P., Kumar, R., Weber, M., Knoll, L., Fleckenstein, J. H., & Musolff, A. (2021). Archetypes and controls of riverine nutrient export across german catchments. *Water Resources Research*, *57*(4). https://doi.org/10.1029/2020WR028134

EEA. (2013). *DEM over Europe from the GMES RDA project (EU-DEM, resolution 25m) - version 1*. E. E. Agency. Retrieved from https://sdi.eea.europa.eu/catalogue/eea/api/records/66fa7dca-8772-4a5d-9d56-2caba4ecd36a

Ehrhardt, S., Kumar, R., Fleckenstein, J. H., Attinger, S., & Musolff, A. (2019). Trajectories of nitrate input and output in three nested catchments along a land use gradient. *Hydrology and Earth System Sciences*, *23*(8), 3503–3524. https://doi.org/10.5194/hess-23-3503-2019

Evans, C., & Davies, T. D. (1998). Causes of concentration/discharge hysteresis and its potential as a tool for analysis of episode hydrochemistry. *Water Resources Research*, *34*(1), 129–137. https://doi.org/10.1029/97wr01881

Foley, J. A., Defries, R. S., Asner, G. P., Barford, C., Bonan, G., Carpenter, S. R., et al. (2005). Global consequences of land use. *Science*, *309*(5734), 570–574. https://doi.org/10.1126/science.1111772

Fovet, O., Humbert, G., Dupas, R., Gascuel-Odoux, C., Gruau, G., Jaffrezic, A., et al. (2018). Seasonal variability of stream water quality response to storm events captured using high-frequency and multi-parameter data. *Journal of Hydrology*, *559*, 282–293. https://doi.org/10.1016/j.jhydrol.2018.02.040

Frei, S., Knorr, K. H., Peiffer, S., & Fleckenstein, J. H. (2012). Surface micro-topography causes hot spots of biogeochemical activity in wetland systems: A virtual modeling experiment. *Journal of Geophysical Research: Biogeosciences*, *117*, G00n12. https://doi.org/10.1029/2012jg002012

Gall, H. E., Park, J., Harman, C. J., Jawitz, J. W., and Rao, P. S. C. (2013). Landscape filtering of hydrologic and biogeochemical responses in managed catchments, *Landscape Ecology*, *28*(4), 651–664, https://doi.org/10.1007/s10980-012-9829-x

Godsey, S. E., Hartmann, J., & Kirchner, J. W. (2019). Catchment chemostasis revisited: Water quality responds differently to variations in weather and climate. *Hydrological Processes*, *33*(24), 3056–3069. https://doi.org/10.1002/hyp.13554

Godsey, S. E., Kirchner, J. W., & Clow, D. W. (2009). Concentration-discharge relationships reflect chemostatic characteristics of US catchments. *Hydrological Processes*, *23*(13), 1844–1864. https://doi.org/10.1002/Hyp.7315

Grubbs, F. E. (1950). Sample criteria for testing outlying observations. *The Annals of Mathematical Statistics*, *21*(1), 27–58. https://doi.org/10.1214/aoms/1177729885

Guillemot, S., Fovet, O., Gascuel-Odoux, C., Gruau, G., Casquin, A., Curie, F., et al. (2021). Spatio-temporal controls of C–N–P dynamics across headwater catchments of a temperate agricultural region from public data analysis. *Hydrology and Earth System Sciences*, *25*(5), 2491–2511. https://doi.org/10.5194/hess-25-2491-2021

Hensley, R. T., Cohen, M. J., & Jawitz, J. W. (2018). Channel filtering generates multifractal solute signals. *Geophysical Research Letters*, *45*(21), 11722–11731. https://doi.org/10.1029/2018gl079864

House, W. A., & Warwick, M. S. (1998). Hysteresis of the solute concentration/discharge relationship in rivers during storms. *Water Research*, *32*(8), 2279–2290. https://doi.org/10.1016/S0043-1354(97)00473-9

Jawitz, J. W., & Mitchell, J. (2011). Temporal inequality in catchment discharge and solute export. *Water Resources Research*, *47*, W00j14. https://doi.org/10.1029/2010wr010197

Kirchner, J. W. (2003). A double paradox in catchment hydrology and geochemistry. *Hydrological Processes*, *17*(4), 871–874. https://doi.org/10.1002/hyp.5108

Kirchner, J. W., Feng, X. H., Neal, C., & Robson, A. J. (2004). The fine structure of water-quality dynamics: The (high-frequency) wave of the future. *Hydrological Processes*, *18*(7), 1353–1359. https://doi.org/10.1002/hyp.5537

Knapp, J. L. A., von Freyberg, J., Studer, B., Kiewiet, L., & Kirchner, J. W. (2020). Concentration-discharge relationships vary among hydrological events, reflecting differences in event characteristics. *Hydrology and Earth System Sciences*, *24*(5), 2561–2576. https://doi.org/10.5194/hess-24-2561-2020

Knorr, K. H. (2013). DOC-dynamics in a small headwater catchment as driven by redox fluctuations and hydrological flow paths - Are DOC exports mediated by iron reduction/oxidation cycles? *Biogeosciences*, *10*(2), 891–904. https://doi.org/10.5194/bg-10-891-2013

Koenig, L. E., Shattuck, M. D., Snyder, L. E., Potter, J. D., & McDowell, W. H. (2017). Deconstructing the Effects of Flow on DOC, Nitrate, and Major Ion Interactions Using a High-Frequency Aquatic Sensor Network. *Water Resources Research*, *53*(12), 10655–10673. https://doi.org/10.1002/2017wr020739

Kong, X. Z., Zhan, Q., Boehrer, B., & Rinke, K. (2019). High frequency data provide new insights into evaluating and modeling nitrogen retention in reservoirs. *Water Research*, *166*, 115017. https://doi.org/10.1016/j.watres.2019.115017

Krueger, T., Quinton, J. N., Freer, J., Macleod, C. J. A., Bilotta, G. S., Brazier, R. E., et al. (2009). Uncertainties in data and models to describe event dynamics of agricultural sediment and phosphorus transfer. *Journal of Environmental Quality*, *38*(3), 1137–1148. https://doi.org/10.2134/jeq2008.0179

LHW. (2018). *Datenportal Gewaesserkundlicher Landesdienst Sachsen-Anhalt (GLD), L. F. H. u. W. Sachsen-anhalt*. Retrieved from https://gld-sa.dhi-wasy.de/GLD-Portal/

Lloyd, C. E. M., Freer, J. E., Johnes, P. J., & Collins, A. L. (2016). Using hysteresis analysis of high-resolution water quality monitoring data, including uncertainty, to infer controls on nutrient and sediment transfer in catchments. *The Science of the Total Environment*, *543*, 388–404. https://doi.org/10.1016/j.scitotenv.2015.11.028

Marinos, R. E., Van Meter, K. J., & Basu, N. B. (2020). Is the river a Chemostat?: Scale versus land use controls on nitrate concentration-discharge dynamics in the Upper Mississippi River Basin. *Geophysical Research Letters*, *47*(16), e2020GL087051. https://doi.org/10.1029/2020GL087051

Minaudo, C., Dupas, R., Gascuel-Odoux, C., Fovet, O., Mellander, P. E., Jordan, P., et al. (2017). Nonlinear empirical modeling to estimate phosphorus exports using continuous records of turbidity and discharge. *Water Resources Research*, *53*(9), 7590–7606. https://doi.org/10.1002/2017wr020590

Minaudo, C., Dupas, R., Gascuel-Odoux, C., Roubeix, V., Danise, P. A., & Moatar, F. (2019). Seasonal and event-based concentration-discharge relationships to identify catchment controls on nutrient export regimes. *Advances in Water Resources*, *131*, 103379. https://doi.org/10.1016/j.advwatres.2019.103379

Moatar, F., Abbott, B. W., Minaudo, C., Curie, F., & Pinay, G. (2017). Elemental properties, hydrology, and biology interact to shape concentration-discharge curves for carbon, nutrients, sediment, and major ions. *Water Resources Research*, *53*(2), 1270–1287. https://doi.org/10.1002/2016WR019635

Musolff, A. (2020a). High frequency dataset for event-scale concentration-discharge analysis, HydroShare. https://doi.org/10.4211/hs.27c93a3f4ee2467691a1671442e047b8

Musolff, A. (2020b). An R code for event analysis of concentration-discharge relationships and hysteresis, HydroShare. https://doi.org/10.4211/hs.dcbd27b20cee4ebcb92436acb94fa6c3

Musolff, A., Fleckenstein, J. H., Opitz, M., Büttner, O., Kumar, R., & Tittel, J. (2018). Spatio-temporal controls of dissolved organic carbon stream water concentrations. *Journal of Hydrology*, *566*, 205–215. https://doi.org/10.1016/j.jhydrol.2018.09.011

Musolff, A., Fleckenstein, J. H., Rao, P. S. C., & Jawitz, J. W. (2017). Emergent archetype patterns of coupled hydrologic and biogeochemical responses in catchments. *Geophysical Research Letters*, *44*(9), 4143–4151. https://doi.org/10.1002/2017GL072630

Musolff, A., Schmidt, C., Rode, M., Lischeid, G., Weise, S. M., & Fleckenstein, J. H. (2016). Groundwater head controls nitrate export from an agricultural lowland catchment. *Advances in Water Resources*, *96*, 95–107. https://doi.org/10.1016/j.advwatres.2016.07.003

Musolff, A., Schmidt, C., Selle, B., & Fleckenstein, J. H. (2015). Catchment controls on solute export. *Advances in Water Resources*, *86*, 133–146. https://doi.org/10.1016/j.advwatres.2015.09.026

Musolff, A., Selle, B., Buettner, O., Opitz, M., & Tittel, J. (2017). Unexpected release of phosphate and organic carbon to streams linked to declining nitrogen depositions. *Global Change Biology*, *23*, 1891–1901. https://doi.org/10.1111/gcb.13498

Nguyen, T. V., Kumar, R., Lutz, S. R., Musolff, A., Yang, J., & Fleckenstein, J. H. (2021). Modeling nitrate export from a mesoscale catchment using storage selection functions. *Water Resources Research*, *57*(2). https://doi.org/10.1029/2020WR028490

Onderka, M., Wrede, S., Rodny, M., Pfister, L., Hoffmann, L., & Krein, A. (2012). Hydrogeologic and landscape controls of dissolved inorganic nitrogen (DIN) and dissolved silica (DSi) fluxes in heterogeneous catchments. *Journal of Hydrology*, *450*, 36–47. https://doi.org/10.1016/j.jhydrol.2012.05.035

Outram, F. N., Cooper, R. J., Sunnenberg, G., Hiscock, K. M., & Lovett, A. A. (2016). Antecedent conditions, hydrological connectivity and anthropogenic inputs: Factors affecting nitrate and phosphorus transfers to agricultural headwater streams. *The Science of the Total Environment*, *545*, 184–199. https://doi.org/10.1016/j.scitotenv.2015.12.025

Raeke, J., Lechtenfeld, O. J., Tittel, J., Oosterwoud, M. R., Bornmann, K., & Reemtsma, T. (2017). Linking the mobilization of dissolved organic matter in catchments and its removal in drinking water treatment to its molecular characteristics. *Water Research*, *113*, 149–159. https://doi.org/10.1016/j.watres.2017.01.066

Richardson, C. M., Zimmer, M. A., Fackrell, J. K., & Paytan, A. (2020). Geologic controls on source water drive baseflow generation and carbon geochemistry: Evidence of nonstationary baseflow sources across multiple subwatersheds. *Water Resources Research*, *56*(7). https://doi.org/10.1029/2019WR026577

Riedel, T., Zak, D., Biester, H., & Dittmar, T. (2013). Iron traps terrestrially derived dissolved organic matter at redox interfaces. *Proceedings of the National Academy of Sciences of the United States of America*, *110*(25), 10101–10105. https://doi.org/10.1073/pnas.1221487110

Rode, M., Halbedel, S., Anis, M. R., Borchardt, D. W., & Weitere, M. (2016). Continuous in-stream assimilatory nitrate uptake from high-frequency sensor measurements. *Environmental Science and Technology*, *50*(11), 5685–5694. https://doi.org/10.1021/acs.est.6b00943

Rode, M., Wade, A. J., Cohen, M. J., Hensley, R. T., Bowes, M. J., Kirchner, J. W., et al. (2016). Sensors in the Stream: The High-Frequency Wave of the Present. *Environmental Science & Technology*, *50*(19), 10297–10307. https://doi.org/10.1021/acs.est.6b02155

Rose, L. A., Karwan, D. L., & Godsey, S. E. (2018). Concentration-discharge relationships describe solute and sediment mobilization, reaction, and transport at event and longer timescales. *Hydrological Processes*, *32*(18), 2829–2844. https://doi.org/10.1002/hyp.13235

Schlesinger, W. H. (2009). On the fate of anthropogenic nitrogen. *Proceedings of the National Academy of Sciences of the United States of America*, *106*(1), 203–208. https://doi.org/10.1073/pnas.0810193105

Sebestyen, S. D., Boyer, E. W., Shanley, J. B., Kendall, C., Doctor, D. H., Aiken, G. R., & Ohte, N. (2008). Sources, transformations, and hydrological processes that control stream nitrate and dissolved organic matter concentrations during snowmelt in an upland forest. *Water Resources Research*, *44*(12), W12410. https://doi.org/10.1029/2008wr006983

Seibert, J., Grabs, T., Kohler, S., Laudon, H., Winterdahl, M., & Bishop, K. (2009). Linking soil- and stream-water chemistry based on a Riparian Flow-Concentration Integration Model. *Hydrology and Earth System Sciences*, *13*(12), 2287–2297. https://doi.org/10.5194/hess-13-2287-2009

Simpson, E. H. (1951). The Interpretation of Interaction in Contingency Tables. *Journal of the Royal Statistical Society: Series B*, *13*(2), 238–241. https://doi.org/10.1111/j.2517-6161.1951.tb00088.x

Sivapalan, M. (2006). Pattern, process and function: Elements of a unified theory of hydrology at the catchment scale. In M. G. Anderson (Ed.), *Encyclopedia of hydrological Sciences*: John Wiley & Sons, Ltd. https://doi.org/10.1002/0470848944.hsa012

Strohmeier, S., Knorr, K. H., Reichert, M., Frei, S., Fleckenstein, J. H., Peiffer, S., & Matzner, E. (2013). Concentrations and fluxes of dissolved organic carbon in runoff from a forested catchment: Insights from high frequency measurements. *Biogeosciences*, *10*(2), 905–916. https://doi.org/10.5194/bg-10-905-2013

Strohmenger, L., Fovet, O., Akkal-Corfini, N., Dupas, R., Durand, P., Faucheux, M., et al. (2020). Multitemporal relationships between the hydroclimate and exports of carbon, nitrogen, and phosphorus in a small agricultural watershed. *Water Resources Research*, *56*(7). https://doi.org/10.1029/2019WR026323

Tarasova, L., Basso, S., Zink, M., & Merz, R. (2018). Exploring controls on rainfall-runoff events: 1. Time series- based event separation and temporal dynamics of event runoff response in Germany. *Water Resources Research*, *54*(10), 7711–7732. https://doi.org/10.1029/2018wr022587

Taylor, P. G., & Townsend, A. R. (2010). Stoichiometric control of organic carbon-nitrate relationships from soils to the sea. *Nature*, *464*(7292), 1178–1181. https://doi.org/10.1038/nature08985

Thompson, S. E., Basu, N. B., Lascurain, J., Aubeneau, A., & Rao, P. S. C. (2011). Relative dominance of hydrologic versus biogeochemical factors on solute export across impact gradients. *Water Resources Research*, *47*. https://doi.org/10.1029/2010wr009605

van der Velde, Y., de Rooij, G. H., Rozemeijer, J. C., van Geer, F. C., & Broers, H. P. (2010). Nitrate response of a lowland catchment: On the relation between stream concentration and travel time distribution dynamics. *Water Resources Research*, *46*, W11534. https://doi.org/10.1029/2010WR009105

Vaughan, M. C. H., Bowden, W. B., Shanley, J. B., Vermilyea, A., Sleeper, R., Gold, A. J., et al. (2017). High-frequency dissolved organic carbon and nitrate measurements reveal differences in storm hysteresis and loading in relation to land cover and seasonality. *Water Resources Research*, *53*(7), 5345–5363. https://doi.org/10.1002/2017wr020491

von Freyberg, J., Studer, B., & Kirchner, J. W. (2017). A lab in the field: High-frequency analysis of water quality and stable isotopes in stream water and precipitation. *Hydrology and Earth System Sciences*, *21*(3), 1721–1739. https://doi.org/10.5194/hess-21-1721-2017

Werner, B. J., Musolff, A., Lechtenfeld, O. J., de Rooij, G. H., Oosterwoud, M. R., & Fleckenstein, J. H. (2019). High-frequency measurements explain quantity and quality of dissolved organic carbon mobilization in a headwater catchment. *Biogeosciences*, *16*(22), 4497–4516. https://doi.org/10.5194/bg-16-4497-2019

Westphal, K., Musolff, A., Graeber, D., & Borchardt, D. (2020). Controls of point and diffuse sources lowered riverine nutrient concentrations asynchronously, thereby warping molar N:P ratios. *Environmental Research Letters*, *15*(10), 104009. https://doi.org/10.1088/1748-9326/ab98b6

Winter, C., Lutz, S. R., Musolff, A., Kumar, R., Weber, M., & Fleckenstein, J. H. (2020). Disentangling the impact of catchment heterogeneity on nitrate export dynamics from event to long-term time scales. *Water Resources Research*, *57*, e2020WR027992. https://doi.org/10.1029/2020WR027992

Winterdahl, M., Erlandsson, M., Futter, M. N., Weyhenmeyer, G. A., & Bishop, K. (2014). Intra-annual variability of organic carbon concentrations in running waters: Drivers along a climatic gradient. *Global Biogeochemical Cycles*, *28*(4), 451–464. https://doi.org/10.1002/2013gb004770

Winterdahl, M., Futter, M., Kohler, S., Laudon, H., Seibert, J., & Bishop, K. (2011). Riparian soil temperature modification of the relationship between flow and dissolved organic carbon concentration in a boreal stream. *Water Resources Research*, *47*, W08532. https://doi.org/10.1029/2010wr010235

Wold, S., Sjostrom, M., & Eriksson, L. (2001). PLS-regression: A basic tool of chemometrics. *Chemometrics and Intelligent Laboratory Systems*, *58*(2), 109–130. https://doi.org/10.1016/S0169-7439(01)00155-1

Wollheim, W. M., Mulukutla, G. K., Cook, C., & Carey, R. O. (2017). Aquatic nitrate retention at river network scales across flow conditions determined using nested in situ sensors. *Water Resources Research*, *53*(11), 9740–9756. https://doi.org/10.1002/2017wr020644

Wollschlager, U., Attinger, S., Borchardt, D., Brauns, M., Cuntz, M., Dietrich, P., et al. (2017). The Bode hydrological observatory: A platform for integrated, interdisciplinary hydro-ecological research within the TERENO Harz/Central German Lowland Observatory. *Environmental Earth Sciences*, *76*(1). https://doi.org/10.1007/s12665-016-6327-5

Yang, J., Heidbuchel, I., Musolff, A., Reinstorf, F., & Fleckenstein, J. H. (2018). Exploring the dynamics of transit times and subsurface mixing in a small agricultural catchment. *Water Resources Research*, *54*(3), 2317–2335. https://doi.org/10.1002/2017wr021896

Zarnetske, J. P., Bouda, M., Abbott, B. W., Saiers, J., & Raymond, P. A. (2018). Generality of hydrologic transport limitation of watershed organic carbon flux across ecoregions of the United States. *Geophysical Research Letters*, *45*(21), 11702–11711. https://doi.org/10.1029/2018gl080005

Zhang, X. L., Yang, X. Q., Jomaa, S., & Rode, M. (2020). Analyzing impacts of seasonality and landscape gradient on event-scale nitrate-discharge dynamics based on nested high-frequency monitoring. *Journal of Hydrology*, *591*, 125585. https://doi.org/10.1016/j.jhydrol.2020.125585

Zhi, W., & Li, L. (2020). The Shallow and deep hypothesis: Subsurface Vertical chemical contrasts shape nitrate export patterns from different land uses. *Environmental Science & Technology*, *54*(19), 11915–11928. https://doi.org/10.1021/acs.est.0c01340

Zhi, W., Li, L., Dong, W. M., Brown, W., Kaye, J., Steefel, C., & Williams, K. H. (2019). Distinct source water chemistry shapes contrasting concentration-discharge patterns. *Water Resources Research*, *55*(5), 4233–4251. https://doi.org/10.1029/2018wr024257